

Network of Excellence

NEWCOM#

Network of Excellence in Wireless Communications#

FP7 Contract Number: 318306



WP22 – Networking technologies for the Internet of Things (IoT) with mobile clouds

D22.4

Final results obtained in the lab infrastructures

Contractual Delivery Date:	October 31, 2015
Actual Delivery Date:	November 20, 2015
Responsible Beneficiary:	CNIT/UniBO
Contributing Beneficiaries:	CNIT/UniBO, CNIT/UniCT, CTTC, CNRS/SUPELEC/UniPS, CNRS/Eurecom, UCL, Bilkent, Stony Brook Univ.
Estimated Person Months:	20
Dissemination Level:	Public
Nature:	Report
Version:	1.0

PROPRIETARY RIGHTS STATEMENT

This document contains information, which is proprietary to the NEWCOM# Consortium.

This page is left blank intentionally

Document Information

Document ID:	D22.4
Version Date:	November 19, 2015
Total Number of Pages:	68
Abstract:	This document describes the final advancements of the JRAs adopting the EuWIN@CNIT-BO site platforms.
Keywords:	EuWin, Laboratory description, Experimental research, CNIT-BO site, Internet of Things, Smart City, Delay Tolerant Networks, Routing, Localization.

Authors

Full Name	Beneficiary / Organisation	e-mail	Role
Davide Dardari	CNIT-Bologna	davide.dardari@unibo.it	Editor
Roberto Verdone	CNIT-Bologna	roberto.verdone@unibo.it	Contributor
Melchiorre Danilo Abrignani	CNIT-Bologna	danilo.abrignani@unibo.it	Contributor
Chiara Buratti	CNIT-Bologna	c.buratti@unibo.it	Contributor
Andrea Stajkic	CNIT-Bologna	andrea.stajkic@unibo.it	Contributor
Stefan Mijovic	CNIT-Bologna	stefan.mijovic@unibo.it	Contributor
Colian Giannini	CNIT-Bologna	colian.giannini@unibo.it	Contributor
Giacomo Calanchi	CNIT-Bologna	giacomo.calanchi@studio.unibo.it	Software developer
Giacomo Morabito	CNIT-Catania	morabito.giacomo@gmail.com	Contributor
Sebastiano Milardo	CNIT-Catania	s.milardo@hotmail.it	Contributor
Riccardo Cavallari	CNIT-Bologna		Contributor
Florian Kaltenberger	CNRS-Eurecom	Florian.kaltenberger@eurecom.fr	Contributor
Miquel Payaro	CTTC	miquel.payaro@cttc.es	Contributor
Vincenzo Zambianchi	CNIT-Bologna	vincenzo.zambianchi@unibo.it	Contributor
Francesca Bassi	CNRS-SUPELEC	francesca.bassi@lss.supelec.fr	Contributor
Michel Kieffer	CNRS-SUPELEC	kieffer@lss.supelec.fr	Contributor
Gianni Pasolini	CNIT-Bologna	gianni.pasolini@unibo.it	Contributor
Carles Fernandez	CTTC	carles.fernandez@cttc.es	Contributor
Pau Closas	CTTC	pau.closas@cttc.cat	Contributor
Achraf Mallat	UCL	achraf.Mallat@uclouvain.be	Contributor
Luc Vandendorpe	UCL	luc.vandendorpe@uclouvain.be	Contributor
Sinan Gezici	Bilkent	gezici@ee.bilkent.edu.tr	Contributor
Petar Djuric	Stony Brook Univ.	petar.djuric@stonybrook.edu	Contributor

Reviewers

Full Name	Beneficiary / Organisation	e-mail	Date
Roberto Verdone	CNIT/UniBO	roberto.verdone@unibo.it	October 8, 2015
Marco Luise	CNIT/UniPI	marco.luise@cnit.it	November 19, 2015

Version history

Issue	Date of Issue	Comments
0.1	June 1, 2015	TOC definition – D. Dardari / R. Verdone
0.2	July 15, 2015	Contribution from partners
0.3	October 8, 2015	Review and integration document – R. Verdone
1.0	November 19, 2015	Final Version

Executive Summary

This document describes the activities performed within WP2.2 during the third year of Newcom#.

The advances and achievements of each active joint research activity (JRA) are summarized in the body of this document. The inter-WP or inter-Track nature of the JRAs is highlighted when present. Technical details about the different JRAs have been included in Annex I.

The activity of the last year have been mainly concentrated in finalizing the experimental campaign using the EuWin@CNIT-BO platforms to validate theoretical results obtained in Track 1.

Within EuWin a particular effort has been devoted to demonstration activities, meetings with industries, workshops, and to the organization of training schools dedicated to experimental research. These dissemination activities are described in Annex II, which is common to the three Deliverables D21.4, D22.4 and D23.4. Starting from this dissemination campaign, collaboration with companies willing to exploit the capabilities of the EuWin platform for experimental research has been established, as reported in this document.

Table of Contents

2. Introduction	8
2.1 Glossary	8
2.2 List of Joint Research Activities (JRAs)	9
2.3 Description of the Main WP Achievements in the Reporting Period.....	9
3. Detailed Activity and Achieved Results	10
3.1 JRA #1 " <i>Design and experimental validation of algorithms for active and passive indoor positioning</i> "	10
3.1.1 Description of Activity	10
3.1.2 Relevance with the identified fundamental open issues	10
3.1.3 Main Results Achieved in the Reporting Period	11
3.1.4 Publications	11
3.2 JRA #3 " <i>Experimental activity on data sensing and fusion</i> " - Evaluation of Distributed Non-Asymptotic Confidence Region Computation over Wireless Sensor Networks	12
3.2.1 Description of Activity	12
3.2.2 Relevance with the identified fundamental open issues	12
3.2.3 Main Results Achieved in the Reporting Period	12
3.2.4 Publications	13
3.3 JRA #3 " <i>Experimental activity on data sensing and fusion</i> " - Experimental verification of distributed fault detection for wireless sensor network	14
3.3.1 Description of Activity	14
3.3.2 Relevance with the identified fundamental open issues	14
3.3.3 Main Results Achieved in the Reporting Period	14
3.3.4 Publications	15
3.4 JRA#5 " <i>Socially-Aware Protocols for Wireless Mesh Networks</i> "	16
3.4.1 Description of Activity	16
3.4.2 Relevance with the identified fundamental open issues	16
3.4.3 Main Results Achieved in the Reporting Period	16
3.4.4 Publications	17
3.5 JRA#6 " <i>Testing IP-based Wireless Sensor Networks for the Internet of Things</i> "	18
3.5.1 Description of Activity	18
3.5.2 Relevance with the identified fundamental open issues	18
3.5.3 Main Results Achieved in the Reporting Period	19
3.5.4 Publications	19
3.6 Industrial Activity	20
3.6.1 Collaboration between CNIT-UniBO and CPL Concordia	20
4. General Conclusions and Prospects.....	23
5. Annex I: Detailed Description of Main Technical WP Achievements	24
5.1 Achievements of JRA#1 " <i>Design and experimental validation of algorithms for active and passive indoor positioning</i> "	24
5.1.1 Low-cost IEEE 802.11.4a ultra-wideband localization platform.....	24
5.1.2 Experimental validation of crowd mapping algorithms	28
5.2 Achievements of JRA#3 " <i>Experimental activity on data sensing and fusion</i> "	33
5.2.1 Evaluation of Distributed Non-Asymptotic Confidence Region Computation over Wireless Sensor Networks	33

5.2.2	Experimental verification of distributed fault detection for wireless sensor network.....	49
5.3	Achievements of JRA#5 "Socially-Aware Protocols for Wireless Mesh Networks"	51
5.3.1	Introduction.....	51
5.3.2	Inter-Contact Time Distribution and Markov Model	51
5.3.3	Epidemic Information Dissemination Model	52
5.3.4	Numerical Evaluation.....	53
5.3.5	Conclusions	56
5.4	Achievements of JRA#6 "Testing IP-based Wireless Sensor Networks for the Internet of Things"	57
5.4.1	Experimental Setup	57
5.4.2	Numerical Results	58
5.4.3	Conclusions	60
6.	Annex II: Integration Document	61
6.1	Introduction	61
6.2	Integration among the sites	61
6.3	Dissemination	62
6.4	Training	63
6.5	Participation to EuCNC 2015.....	64
6.6	Plans after Year 3	66
6.7	Plans for the Future	66
6.8	Conclusions	67

1.Introduction

1.1 Glossary

6LoWPAN	Low-Power Wireless Personal Area Networks
AEF	Aggregation Equivalent Flow
AGGR	Aggregation Layer
AODV	Ad hoc On-Demand Distance Vector
AP	Access point
DFD	Distributed fault detection
DIO	Information Object
DIS	Information Solicitation
DODAG	Destination-Oriented Directed Acyclic Graph
FWD	Forwarding Layer
GP	Gaussian process
HGI	Home Gateway Initiative
IMU	Inertial measurement unit
IoT	Internet of Things
LWN	Linear Wireless Network
LWSN	Linear Wireless Sensor Network
MAC	Medium Access Control
FL	Modified flooding
MTO	Many-To-One
MTO-RR	Route Request
NOS	Network Operating System
PER	Packet error rate
PLR	Packet loss rate
RMSE	root mean square error
RREP	Route Replay packet
RREQ	Route Request packet
RSS	Received signal strength
RTT	Round-trip-time
RV	Random variable
SDN	Software Defined Networking
SDWN	Software Defined Wireless Networking
SPS	Sign Perturbed Sums
SR	Source Routing
TAS	Tagged and aggregated sums
TDOA	Time-difference-of-arrival
TOA	Time-of-arrival
TTL	Time To Live
UWB	Ultrawide bandwidth
WSN	Wireless Sensor Network
ZC	Zigbee Coordinator
ZED	Zigbee end-device

1.2 List of Joint Research Activities (JRAs)

This is the list of JRAs that have been planned at the beginning of the NoE, with the corresponding actual status at time of writing:

- JRA#1, "Design and experimental validation of algorithms for active and passive indoor positioning": This JRA is active and its results are reported in Section 2.1 and Annexes 4.1.
- *JRA #2 not active*
- JRA#3, "Experimental activity on data sensing and fusion": This JRA is active on two separate sub-lines and its final results are reported in Sections 2.2 and 2.3 and Annex 4.2.
- JRA#4, "*Reducing Traffic Congestion in Wireless Mesh Networks*": This JRA is not active anymore and could be considered as closed.
- JRA#5, "*Socially-aware protocols for wireless mesh networks*": This JRA started during the second year and final results are reported in Section 2.4 and Annex 4.3.
- JRA#6, "Testing IP-based Wireless Sensor Networks for the Internet of Things": This JRA is active and its results are reported in Section 2.5 and 4.4.

1.3 Description of the Main WP Achievements in the Reporting Period

The main achievements of the WP during the third year of Newcom# can be summarized as follows:

- Final integration of the ultra-wideband localization using IEEE 802.11.4a devices into the LOCTEST platform.
- Finalization of the experimental research within the joint research activities (JRAs) carried out using the EuWIn platforms. As will be detailed in the subsequent sections, some JRAs are inter-WP and inter-Track. The former are oriented to increase the integration between the distributed EuWIn laboratories. The latter demonstrates the utility of EuWIn for the experimental validation of theoretical schemes investigated in Track 1. In particular, among the active JRAs, JRA#1 deals with localization issues and mainly uses the LOCTEST platform; JRA#3 is related to efficient and distributed fault detection and information diffusion techniques for wireless sensor networks and it exploits the DATASENS facility. Finally, multi-hop routing protocols and topologies have been studied and tested in JRA#5 and JRA#6 using FLEXTOP.
- Establishment of activities developed in collaboration with industries outside the network of excellence NEWCOM#.
- Dissemination activities in the form of papers, workshops, tutorials and other events (described in Annex II).

2. Detailed Activity and Achieved Results

In this Section we report the main objectives and results obtained in the third year with reference to the active JRAs, namely JRA#1, JRA#3, JRA#5 and JRA#6. Technical details can be found in Annex I.

2.1 JRA #1 “*Design and experimental validation of algorithms for active and passive indoor positioning*”

Davide Dardari (CNIT-BO)

Pau Closas (CTTC)

Carles Fernandez (CTTC)

Sinan Gezici (Bilkent)

Luc Vanderdorpe (UCL)

Achraf Mallat (UCL)

Petar Djuric (Stony Brook Univ.)

2.1.1 *Description of Activity*

The main activities carried out in this JRA are here summarized:

- Finalization of a low-cost IEEE 802.11.4a ultra-wideband (UWB) localization platform working also in time-difference-of-arrival (TDOA) mode;
- Development of a combined Gaussian process - state space method for efficient crowd mapping and its experimental validation (CNIT-BO) [2];
- Teoretical characterization of the threshold regions in time-of-arrival (TOA) estimation and corresponding signal waveform optimization (UCL, Bilkent, CNIT-BO) [3-4];
- Writing of a survey paper on indoor tracking and localization methods and technologies appeared on IEEE Trans. on Vehicular Technologies (special section). (CTTC, CNIT-BO, Stony Brook Univ.) [1].

This JRA is cross WP, WP2.1 and WP2.2, as it involves the EuWIn sites at CTTC and CNIT-BO (LOCTEST and DATASENS platforms).

2.1.2 *Relevance with the identified fundamental open issues*

Indoor localization and tracking is still a challenging problem as it might involve the adoption of heterogeneous technologies providing positioning-dependent measurements such as received signal strength (RSS), signal time-of-arrival (TOA), geomagnetic field, etc.

Therefore theoretical investigations and experimental validation have to be conducted synergically. Indeed the availability of platforms implementing different technologies, such as those developed and set up in EuWIn, represents an added value in this perspective.

For this purpose, the third year of Newcom# has been devoted to the design and implementation of a low-cost UWB localization network based on recently available IEEE 802.11.4a chips. Differently from other existing networks, this one is able to work in TDOA mode without requiring cable synchronization between anchor nodes and using extremely low-cost infrastructures. This allows higher refresh rates and number of simultaneously tracked tags as well as a self-configuring set up. Such a network have been integrated in the

EuWin@UniBO Loctest platform that, together to the EuWin@CTTC platform, gives the possibility to test experimentally localization algorithm developed within the NEWCOM# community and outside under common interfaces and conditions. This will ease the performance assessment and comparison.

The activity related to crowd mapping has brought the development of an efficient algorithm for spatial fields representation whose complexity and memory requirements do not depend on the number of data measured [2]. This makes the proposed solution particularly appealing for crowd mapping applications where a huge amount of data is expected to be collected in random locations. The method has been validated through an experimental campaign involving a high accuracy positioning system and a magnetic mobile sensor as data collector.

Finally, theoretical investigations on mean square error approximations in TOA estimation have been carried out with the purpose to compute the thresholds of the signal to noise ratio a priori region where estimation is useless, threshold and ambiguity regions where an intermediate accuracy is achieved, and the asymptotic region where the Cramer-Rao lower bound is achieved [3-4]. Analytic expressions of the thresholds have been also derived. Such expressions are useful to drive practical and experimental implementations and validation of time based ranging systems.

2.1.3 Main Results Achieved in the Reporting Period

The localization platform available at EuWin@CNIT-BO now includes all main technologies exploitable to provide indoor positioning ranging from RSS, inertial, geomagnetic to ultra-wideband TOA measurements. The whole activity carried out so far involved both staffs from CNIT-BO and CTTC, both for the platform deployment task and for the algorithm development. From a hardware/software viewpoint the job has been accomplished, the platform is ready to be used in the field to take measurements.

The platform has been tested with particle filter based algorithms that feature data-fusion to process data coming from heterogeneous sensors as well as for mapping purposes of geomagnetic and RSS fields.

2.1.4 Publications

- [1] D. Dardari, P. Closas, and P. M. Djuric, "Indoor tracking: Theory, methods, and technologies," IEEE Trans. Veh. Technol., vol. 64, no. 4, pp. 1263–1278, April 2015.
- [2] D. Dardari, A. Arpino, F. Guidi, and R. Naldi, "A combined GP-State space method for efficient crowd mapping," in IEEE ICC 2015 - Workshop on Advances in Network Localization and Navigation (ICC'15 - Workshop ANLN), London, United Kingdom, Jun. 2015.
- [3] A. Mallat, S. Gezici, D. Dardari, C. Craeye, and L. Vandendorpe, "Statistics of the MLE and approximate upper and lower bounds - part I: Application to TOA estimation," IEEE Trans. Signal Process., vol. 62, no. 21, pp. 5663–5676, Nov 2014.
- [4] A. Mallat, S. Gezici, D. Dardari, and L. Vandendorpe, "Statistics of the MLE and approximate upper and lower bounds - part II: Threshold computation and optimal pulse design for TOA estimation," IEEE Trans. Signal Process., vol. 62, no. 21, pp. 5677–5689, Nov 2014.

The last 2 publications resulted the winners of the 2014 Newcom# best paper award.

2.2 JRA #3 "Experimental activity on data sensing and fusion" - Evaluation of Distributed Non-Asymptotic Confidence Region Computation over Wireless Sensor Networks

Alex Calisti (CNIT-BO)

Gianni Pasolini (CNIT-BO)

Francesca Bassi (CNRS-SUPELEC)

Michel Kieffer (CNRS-SUPELEC)

Davide Dardari (CNIT-BO)

Vincenzo Zambianchi (CNIT-BO)

2.2.1 Description of Activity

The computation of confidence regions is very important in many applications, even if it has been less considered in literature. Classical Cramer-Rao-like bounds or application of Kalman filtering are usually analyzed but they need strong assumptions on measurement noise and a good characterization of confidence regions is only possible for a large number of measurements. The Sign Perturbed Sums (SPS) method allows a central unit to derive a confidence region, from a finite set of measurements, and obtain the exact probability that the true parameter value is evaluated. A distributed version of the SPS algorithm and a novel information diffusion strategy, named tagged and aggregated sums (TAS), was presented and compared to other information diffusion strategies, in particular with the modified flooding algorithm (FL).¹ Our aim is to verify the use of this algorithm in a real environment and compare the results with the simulation results obtained in MATLAB. TAS and FL algorithms have been implemented on CC2530 nodes available in the FLEXTOP and DATASENS platforms at EuWIn@CNIT/Bologna. The impact of the protocol stack and of real propagation conditions on the performance of these algorithms have been considered. A large number of experimentations have been performed in order to validate the simulation results in different network topologies.

2.2.2 Relevance with the identified fundamental open issues

This work is an inter-track joint research activity. Two tasks are connected to this JRA: one belonging to Track 1, on the experimental validation of information diffusion schemes for distributed non-asymptotic confidence region computation, the second to Track 2 on energy-efficient data collection and estimation in wireless sensor networks, respectively:

Task 1.3.1B: on energy-efficient data collection and estimation in wireless sensor networks.

Task 2.2.2: Large-scale wireless sensor networks: routing protocols and network topologies.

2.2.3 Main Results Achieved in the Reporting Period

Fifth nodes were been used to evaluate the algorithm in a real environment and to analyze the impact of the MAC layer on system performance. Nodes were placed with a distance of 2 meters between them in an area of $29.50 \times 9 \text{ m}^2$, along the CNIT-WiLab laboratory. Some parameters were managed to see the effect of the MAC layer to the system and the change of the system varying the number of neighbors. Results show how the FL algorithm works

¹ V. Zambianchi, M. Kieffer, F. Bassi, G. Pasolini and D. Dardari, "Distributed SPS algorithms for non-asymptotic confidence region evaluation," Networks and Communications (EuCNC), 2014 European Conference on, pp.1,5, June 2014.

better in unstructured networks also if the impact of real environment and, in particular, of the MAC layer introduce some informations losses. On the contrary, results also underline how TAS algorithm works better in structured networks even though collisions are present.

2.2.4 Publications

A joint publication is under preparation.

2.3 JRA #3 "Experimental activity on data sensing and fusion" - Experimental verification of distributed fault detection for wireless sensor network

Wenjie Li (CNRS-SUPELEC)

Gianni Pasolini (CNIT-BO)

Francesca Bassi (CNRS-SUPELEC)

Michel Kieffer (CNRS-SUPELEC)

Davide Dardari (CNIT-BO)

2.3.1 *Description of Activity*

To preserve the functionality of the wireless sensor network (WSN), it is important to detect the defective sensor nodes that provide measurement outliers. Recently, we proposed a low complexity distributed fault detection (DFD) algorithm for large WSNs in [1]. Different from the classical solutions in the literature which focused on the strategy of local outlier detection test, our approach aims at performing the DFD in an economic way by reducing the complexity of the decision rule and reducing the communication overhead.

Our aim is to use the experimental facilities available within EuWIn@CNIT/Bologna. Compared to the theoretical analysis, the impact of the protocol stack and of real propagation conditions on the performance of the DFD algorithm have been considered. Thanks to its low complexity, the algorithm is not difficult to be implemented on the node CC2530. A large number of experimentations are essential to validate the simulation results.

This experimental activity has seen a researcher mobility from CNRS-SUPELEC-Univ.PS to CNIT-BO in the period June-July 2015.

2.3.2 *Relevance with the identified fundamental open issues*

This work is related to two tasks one belonging to Track 1, the second to Track 2, and hence it is an inter-track joint research activity, respectively,

Task 1.2.3: Energy-efficient data collection in sensor networks.

Task 2.2.2: Large-scale wireless sensor networks: routing protocols, network topologies and cooperative localization.

The experimental activities help us in characterizing the impact of MAC in real scenarios.

2.3.3 *Main Results Achieved in the Reporting Period*

Twenty nodes have been used in the first stage of the experimental activity. Every node is assigned some random virtual position to create the set of neighbors. The performance of different versions of algorithm as a function of total execution time has been characterized as reported in Section 4.2.2.

2.3.4 Publications

- [1] W. Li, F. Bassi, D. Dardari, M. Kieffer, G. Pasolini, "Low-Complexity Distributed Fault Detection for Wireless Sensor Networks", IEEE ICC'15, London, UK, 2015.
- [2] W. Li, F. Bassi, D. Dardari, M. Kieffer, G. Pasolini, "Iterative Distributed Outlier Detection for Wireless Sensor Networks: Equilibrium and Convergence Analysis", Submitted to 54th IEEE Conference on Decision and Control, 2015.
- [3] W. Li, F. Bassi, D. Dardari, M. Kieffer, G. Pasolini, "Distributed outlier detection for Wireless Sensor Networks", Submitted to IEEE Trans. on Signal and Information Processing over Networks, 2015.

2.4 JRA#5 "Socially-Aware Protocols for Wireless Mesh Networks"

Laura Galluccio (CNIT-CT)

Chiara Buratti (CNIT-BO)

Colian Giannini (CNIT-BO)

Roberto Verdone (CNIT-BO)

2.4.1 Description of Activity

New emerging paradigms (e.g., Delay Tolerant Network) try to exploit users' social habits and mobility patterns in order to enable the communication. A lot of theoretical studies presented in the literature are dedicated to derive statistics and property of users' mobility. However, as the best of our knowledge, there exist just few experimental results, due to the lack of real mobility traces and datasets to validate theoretical results.

The aim of this JRA is to use Datasens, one of the facilities provided by EuWin@CNIT/Bologna, to gather experimental mobility traces in a conference environment. These experimental results can be used as input to:

- validate theoretical results proposed in literature
- study and model users' social habits and mobility in conference environment
- simulate routing protocol for Delay Tolerant Networks, using real mobility traces.

2.4.2 Relevance with the identified fundamental open issues

This work is a joint research activity related to Task 1.2.2.

2.4.3 Main Results Achieved in the Reporting Period

Fourty 802.15.4 compliant devices (of the testbed Datasens) were given to attendees to the conference EuCNC 15 held in Paris in June 2015. Upon reception of a periodic beacon sent by each device, all the receiving devices were recording: i) a timestamp, ii) the received power and iii) the ID of the transmitting node. Post processing of gathered data has led to the characterization of the Inter Contact Time among people moving in the conference environment. Moreover, the participants to the experiment were asked to fill a questionnaire that helped the characterization of social behavior of the participants.

Examples of the aforementioned results are reported in Figure 2-1:

- On the left it is plotted the Inter Contact Time distribution (in blue) and the approximating Generalized Pareto Distribution (in red) whose parameter are reported in the figure together with the Root Mean Squared Error.
- On the right it is shown the contact graph of the participants to the experiment. Colors define communities, node dimension highlights the node degree and edge thickness represents the edge weight intended as the number of contacts between the edge ends.

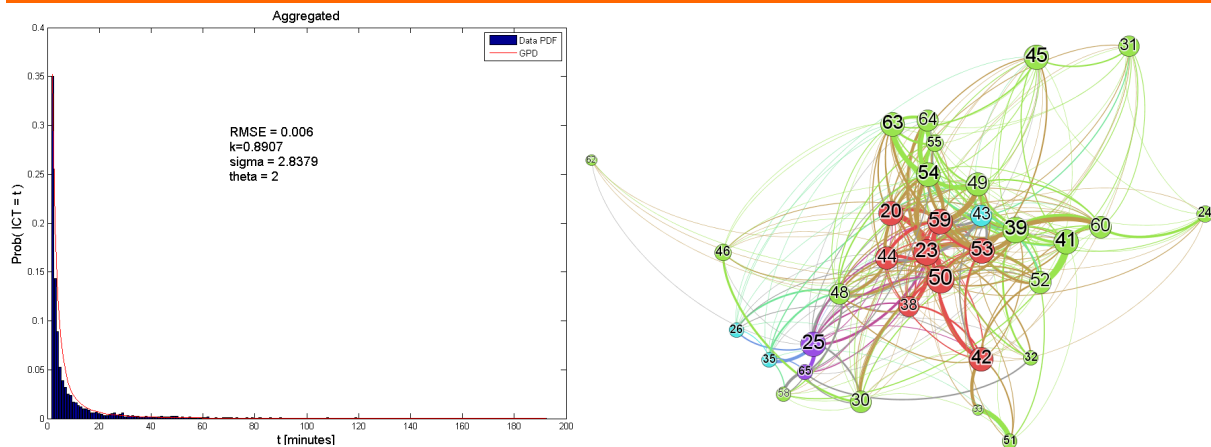


Figure 2-1: PDF of Inter Contact Time and approximation (left)
Social (contact) graph and communities (right)

2.4.4 Publications

- [1] L. Galluccio, C. Giannini, B. Lorenzo, S. Glisic, C. Buratti, R. Verdone, "Epidemic information dissemination in opportunistic scenarios: a realistic model obtained from experimental traces", ISWCS'2015, Brussels, Belgium, 2015
- [2] L. Galluccio, B. Lorenzo, S. Glisic, C. Buratti, C. Giannini, R. Verdone, "Epidemic information dissemination in opportunistic scenarios: a realistic model", EUCNC2015, Paris, France, 2015

2.5 JRA#6 "Testing IP-based Wireless Sensor Networks for the Internet of Things"

Danilo Abrignani (CNIT-BO)

Andrea Stajkic (CNIT-BO)

Stefan Mijovic (CNIT-BO)

Chiara Buratti (CNIT-BO)

Roberto Verdone (CNIT-BO)

Sebastiano Milardo (CNIT-CT)

Giacomo Morabito (CNIT-CT)

Gordana Gardasevic (University of Banja Luka)

2.5.1 Description of Activity

This Joint Research Activity is among CNIT/UniBO, CNIT/UniCT and an external partner that is the University of Banja Luka.

The objective of the JRA was to compare three different solutions for the implementation of the Internet of Things (IoT): i) the Zigbee standard; ii) the IPv6 over Low-Power Wireless Personal Area Networks (6LoWPAN) standard and iii) a proprietary solution based on the Software Defined Networking (SDN) paradigm, called Software Defined Wireless Networking (SDWN). The first two solutions are standard de-facto for Wireless Sensor Networks (WSNs) and implement a distributed re-active routing protocol, while the third solution is based on a centralized proactive routing protocol.

The EuWIn facility used in this JRA is FLEXTOP.

We refer to Deliverable D2.2.3 for details about the implemented solutions, while results of the activity are reported in Appendix 4.4.

2.5.2 Relevance with the identified fundamental open issues

The Internet of Things (IoT) is an emergent paradigm that deals with things (objects, cars, etc.), equipped with radio devices and unique IP addresses. The most used protocol stacks for the above mentioned approaches are 6LoWPAN and Zigbee, respectively. The selection of the best solution, between these two, is still an open issue. Some works in the literature, in fact, provide qualitative comparison between the two standards, while few works deal with comparison of the performance through experimentations, considering very small networks.

More recently a third approach, based on the Software Defined Networking (SDN) paradigm, has been proposed. It is called Software Defined Wireless Networking (SDWN) and it uses a centralized routing protocol. The coordinator/gateway gathers information on the status of the network of things, and brings this knowledge to a controller which can decide on the exploitation of resources within the wireless network. This controller has a centralized vision over the network of things, and can even control things that lie behind several coordinators/gateways. This approach brings the potential advantage of an optimal resource exploitation, even if it could introduce a significant overhead due to signaling back and forth from the controller to the things through the gateway.

The SDWN approach is compared to the distributed approaches as never done in the literature.

2.5.3 Main Results Achieved in the Reporting Period

The three mentioned solutions, implemented on the Texas Instruments (TI) CC2530 devices of the FLEXTOP platform, have been compared through a large measurement campaign, carried out at the University of Bologna. Different performance metrics have been measured and the comparison has been done considering different network topologies, payload sizes and environmental conditions. Some of the achieved results are reported in the Appendix. Results show that in static and quasi-static channel conditions SDWN outperforms the other solutions, independently on the network size, payload size, traffic generated, and performance metric considered. The reason for this is the fact that SDWN allows to optimise paths selection and minimise forwarding time at routers. However, SDWN presents some limitations when high dynamic environments are considered, because of the time needed to refresh paths. As a conclusion, we can state that SDWN is more suitable for applications where nodes are in fixed positions and under low mobility scenario, as for the case of smart home and buildings applications. However, when the situation is dynamic and there is a node mobility, a distributed solutions like ZigBee and 6LoWPAN could work better. As an example, the case of smart city applications, where nodes could be mounted over lamp posts in streets where object (e.g., cars and people) are moving around, or where nodes could be directly carried by moving objects, requires solutions characterised by high reactivity rather than lower delays.

2.5.4 Publications

C. Buratti, A. Stajkic, G. Gardasevic, S. Milardo, D. Abrignani, S. Mijovic, G. Morabito, R. Verdone, "Testing Protocols for The Internet of Things on The EuWIn Platform", accepted for publication to IEEE Journal on Internet of Things, 2015.

2.6 Industrial Activity

2.6.1 Collaboration between CNIT-UniBO and CPL Concordia

This collaboration started in the framework on an Italian project, called “RIGERS - City Regeneration: smart buildings and grids”, participated by CNIT\UniBo and by the Italian SME CPL Concordia. The aim of the project is to create an integrated system for the regeneration of buildings and utility networks, in order to increase the quality of life of citizens. One of the main goals is to develop a platform able to store and manage data related to the state and the consumption of all kind of utilities of buildings.

To the latter aim, CPL Concordia committed to UniBO a series of measurements to be performed over the EuWIn platform at the University of Bologna, FLEXTOP. In particular, UniBO has “reproduced” the building/apartment environment, which is the RIGERS reference scenario, into FLEXTOP, in order to test the intended application, when using IEEE 802.15.4 devices and the Zigbee protocols stack for the upper layers. Some of the achieved results are reported below.

2.6.1.1 Project Description

The collection of data inside buildings require the deployment of huge amount of sensors and the design of proper radio networks able to sustain the offered data traffic.

Each building is characterized by N units (e.g, flat or offices) equipped with a Unit Concentrator (UC). Moreover, a Building Concentrator (BC), in charge of collecting all the data coming from the whole building, is placed on the rooftop. According project specifications each unit is composed of 6 rooms and each room is equipped with 8 sensors (see Figure 2-2 and Table 2-1).

A third element, called Power meter Concentrator (PmC), collects data on power consumption of each unit; note that a differentiation between UC and PmC is needed since usually power meters are not inside the unit itself. Furthermore, there are several sensors deployed in the building (Building Sensors) collecting environmental data. Without giving details about PmC and building sensors, they provide a daily throughput estimated in 13 kB/day per units for PmC and 120 kbit/day for building sensors.

It is possible to identify three levels of nodes (see

Figure 2-3):

- Level 0: BC
- Level 1: UC, PmC and Building Sensors
- Level 2: Unit Sensors.

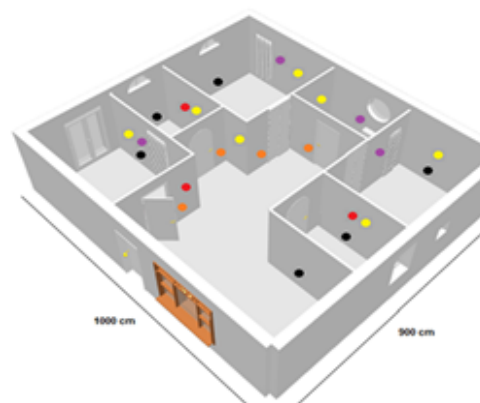


Figure 2-2: The RIGERS reference scenario

Sensors per room	Daily offered throughput
1 hygrometer	2.16 kB/gg
2 temperature sensors	4.32 kB/gg
1 luminosity sensor	2.16 kB/gg
1 presence detector	2.16 kB/gg
1 CO ₂ sensor	2.16 kB/gg
2 radiator consumption sensors	4.32 kB/gg
Total per room	17.28 kB/gg
Total per unit (N = 12)	103.68 kB/gg

Table 2-1: RIGERS sensors

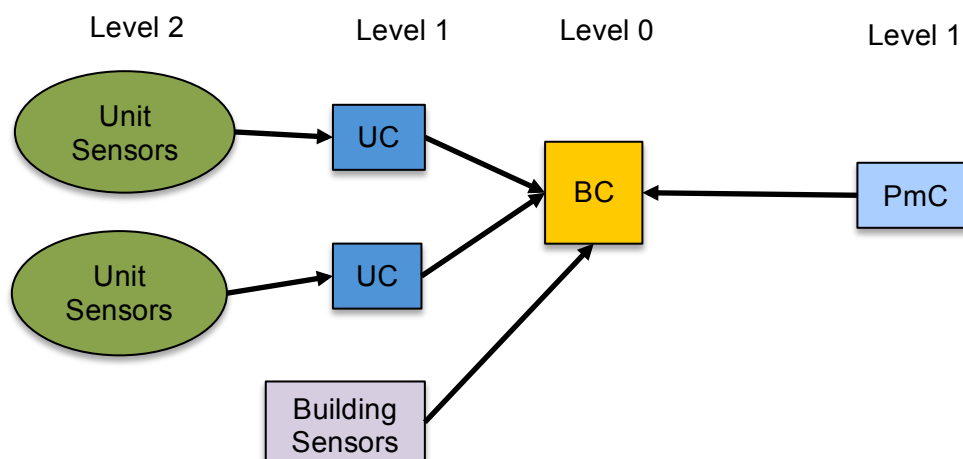


Figure 2-3: The RIGERS architecture

The transmission of data toward the BC can be done through Ethernet connection when such a wired backbone is already present in the building or through a Wireless Sensor Network (WSN). In the latter case the standard considered is 802.15.4/Zigbee.

The communication from Unit Sensors and the respective UC is always done by means of an 802.15.4/Zigbee WSN. Notice, that the connectivity between UC, Building Sensors and PmC with BC is assumed. If it is not the case it is possible to consider more BC per building placed where needed to guarantee the previous assumption.

Furthermore, as the number of unit increases it is possible to have interference among different UCs, in this case an accurate frequency channel assignment has to be performed.

2.6.1.2 Preliminary Experimental Results

As preliminary results the design of the WSN composed by the Unit Sensors and a UC was made both analytically and through experimentation on FLEXTOP.

According to our analysis, in a worst case scenario where Unit Sensors need 3 hops to reach the UC, the 802.15.4/Zigbee WSN is able to cope with an offered traffic of 20 kbit/s. As can be derived from Table 2-1, the traffic offered to the UC amounts to 35kbit/h. Obviously, if all the sensors were synchronized transmitting simultaneously every hour it would not be

possible to sustain the offered traffic with 20kbit/s of capacity. However, if we consider the traffic distributed in a time window which is a design parameter, the traffic can be sustained without any problem. In particular, we estimated that a time window of 15 seconds reduces the offered traffic to 2kbit/sec.

For what concerns the experimental results, we recreated on Flextop the sensors distribution in a unit (see Figure 2-4), by deploying 40 sensors in clusters to simulate a room. Nodes underlined in red in Figure 2-4 are those selected for the experiments.



Figure 2-4: The RIGERS scenario implemented in FLEXTOP.

Below is reported an example of results where we compare the Packet Loss Rate (PLR) per node (considering the 40 deployed nodes) when the transmitting power of nodes is set to 5dBm or to 20dBm. The measurements were done during the night when no people are around, other set of measurements (here not present for sake of brevity) were done during the day to appreciate the effect of people passing by. The graphs show the Per Node-PLR and the total PLR. It is possible to see the worsening in performance passing by a transmitting power of 5 dBm to 20dBm. Moreover, nodes with lower ID (nodes far from the UC) tend to have a higher PLR.

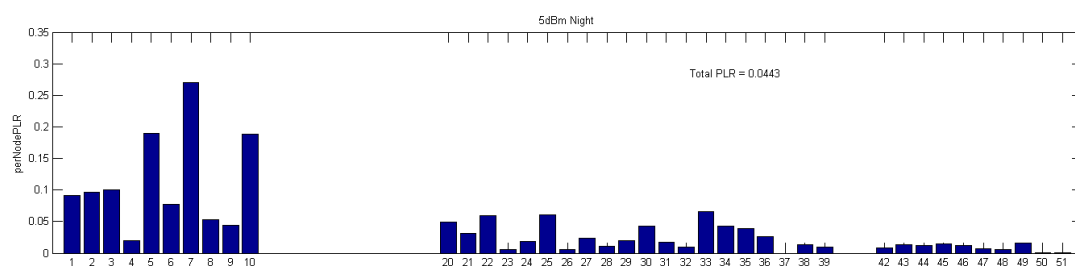


Figure 2-5: Per node PLR when transmitting at 5 dBm.

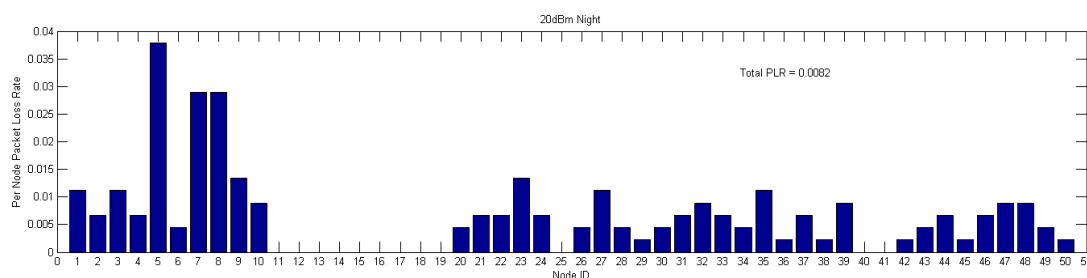


Figure 2-6: Per node PLR when transmitting at 20 dBm.

3. General Conclusions and Prospects

While the second year of activity has been mainly oriented to the launch and consolidation of JRAs, during the third year the experimental research activity enforced the synergy with the theoretical activity developed in Track 1, as described in this document.

Result obtained confirmed how experimental activity is of paramount importance to support and validate theoretical research in real world environments. Indeed, the availability of common and open platforms, such those set up and offered at EuWin sites, has facilitated this process and has given the opportunity for an easier networking among European research groups.

The intense exploitation activity has produced some relevant results, as witnessed by the activity performed on behalf of some companies, such as NEC and Concordia CPL, that requested a number of tests performed over the EuWin@CNIT-BO platform.

4. Annex I: Detailed Description of Main Technical WP Achievements

In this section we report details about results achieved in JRA#1, JRA#3, JRA#5 and JRA#6.

4.1 Achievements of JRA#1 “*Design and experimental validation of algorithms for active and passive indoor positioning*”

4.1.1 Low-cost IEEE 802.11.4a ultra-wideband localization platform

The third year of Newcom# has been devoted to the design and implementation of a low-cost UWB localization network based on recently available IEEE 802.11.4a chips. Differently from other existing networks, this one is able to work in TDOA mode without requiring cable synchronization between anchor nodes and using extremely low-cost infrastructures. This allows higher refresh rates and number of simultaneously tracked tags as well as a self-configuring set up. Such a network have been integrated in the EuWIn@UniBO Loctest platform that, together to the EuWIn@CTTC platform, gives the possibility to test experimentally localization algorithm developed within the NEWCOM# community and outside under common interfaces and conditions. This will easy the performance assessment and comparison. The solution is based on the new UWB chipset DWM1000 realized by Decawave. The chipset DWM1000 enables the location of objects by ensuring a ranging precision below 10 cm, high data rate communications, up to 6.8 Mb/s, and a communication range of several tens of meters (a maximum of 300 meters is declared in ideal situation and considering a slow data rate). The physical layer implemented by the DW1000 follows the standard defined by the IEEE 802.15.4a-2007. This is key point for having a product capable of operating with devices coming from different producers.

The DWM1000 chip has been interfaced with a Raspberry Pi 2 module, where a dedicated firmware allows the communication with the UWB chipset. These boards, managing the operation of the UWB chips, collect the measurements taken from the devices and forward them to a central unit (a computer), which is the core of the localization system. In fact, the central unit determines the position of all the agents present in the monitored environment and returns it to the end user (or, in the case of an automatic detection system, to the network of vehicles in case of a potential collision detection).



Figure 4-1 The Raspberry Pi 2 micro-PC adopted as anchor nodes.

This system developed at CNIT-UNIBO, named SEQUITUR, is based on the Time-Difference-of-Arrival (TDOA) principle, according to which an agent sends UWB signals and the network of anchors determines what is the time difference between the arrival time of the received signal at different nodes. Notice that these radio signals travel at the speed of light so, in a typical application where the localization is performed in an environment of some meters, time differences in the order of few nanoseconds must be computed. Such a scheme needs a perfectly synchronous network of anchors, and then a dedicated algorithm has been designed to this purpose. In particular the anchors continuously exchange UWB packets to reach and maintain a perfect synchronism, necessary to properly measure the time differences between the arrival instants of the agents' signals and to counteract the drift of anchors' internal clock. The main advantage of such a technique, with respect to the standard trilateration previously described (an usually implemented in the other commercial systems), is the higher network throughput, translating in a greater localization update rate (i.e., the number of agent location estimates available per second). In fact, since it is not necessary to determine the distances between each agent and each anchor, a larger number of signals can be sent, with a consequent increasing speed of the algorithms. This is fundamental in all the contexts where the agent moves with a speed not negligible, as happens for the road users. Another key advantage of TDOA-based localization schemes is that the agent's device could be equipped only with a transmitting section so that to drastically reduce its cost and energy consumption (longer battery duration). To this purpose, the system has been designed also to support the 12 bytes blink packet defined by the ISO/IEC 24730-62:2013 air-interface standard for RTLS systems.

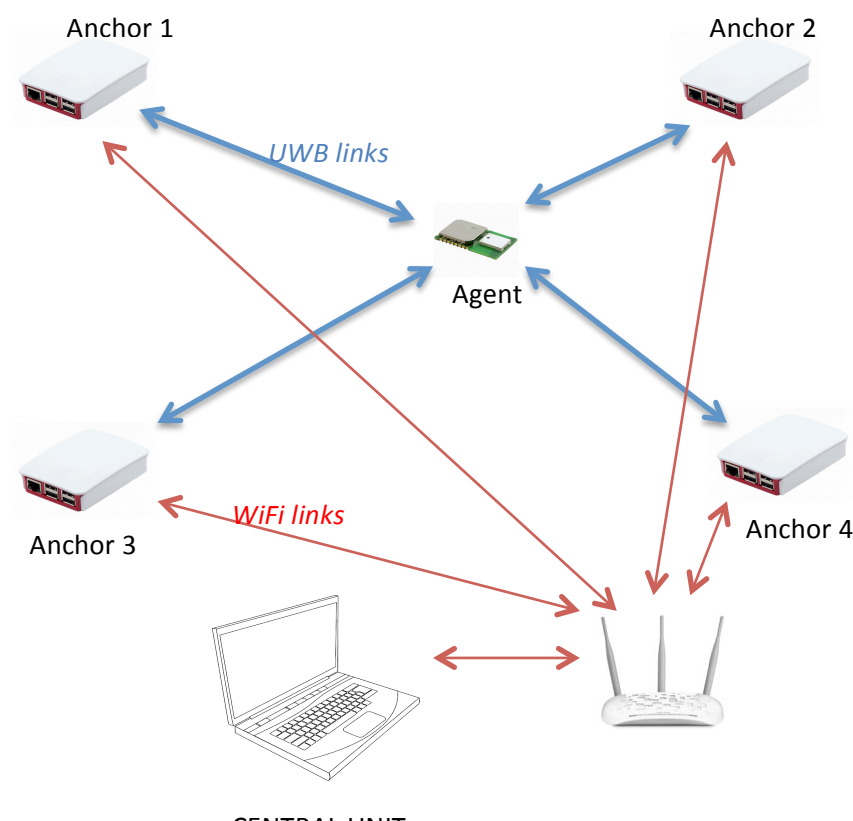


Figure 4-2 The SEQUITUR UWB RTLS

The experimental validation of the system has been carried out in the CASY (Center for Complex Automated Systems) flight arena at the University of Bologna, Cesena campus,

shown in Figure 4-8. The laboratory is equipped with a motion tracking system composed of 22 infrared cameras (VICON Bonita 10) each one characterized by 1 Mpixel resolution. The overall system is able to localize targets within a tracking volume of $(11 \times 11 \times 11) \text{m}^3$ with less than 0.5 mm accuracy at 250 Hz. Such extremely high positioning accuracy allows to consider position errors negligible and use the vision system as a benchmark to validate the performance of radio-based localization systems.

In addition to indoor validation tests, some preliminary tests have been conducted in an outdoor environment where agents moving in a squared area of 20x20m have been successfully tracked without the use of GPS signals and with an accuracy of about 20-30 cm. As shown in Figure 4-3 -- Figure 4-6, both humans and drones have been used as moving agents.

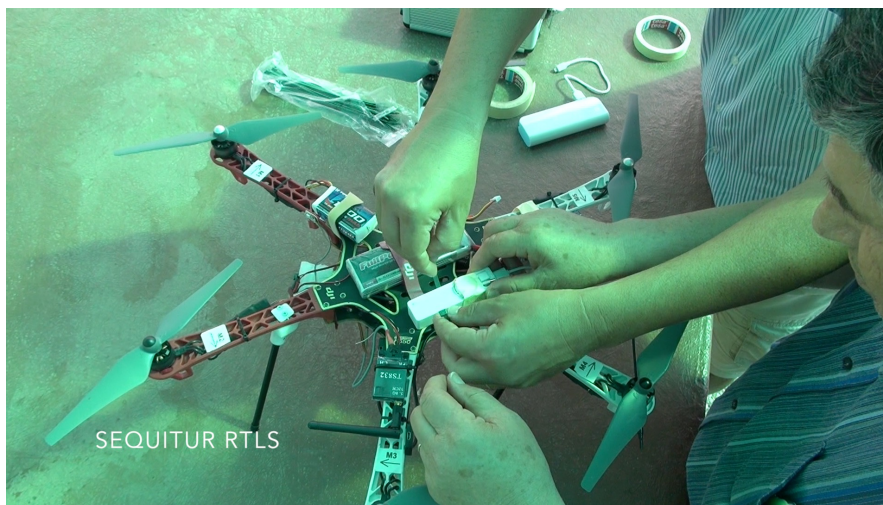


Figure 4-3: Set up phase of UWB tags on drone



Figure 4-4: Tracking of drones using UWB signals



Figure 4-5: Tracking of drones using UWB signals



Figure 4-6: Tracking of humans using UWB signals

4.1.2 Experimental validation of crowd mapping algorithms

4.1.2.1 Introduction

Recently, the crowd sensing concept has been proposed for zero-effort automatic indoor mapping of physical fields using various sensors already embedded in smartphones.

In crowd mapping, empirical data collected by mobile users moving in the environment (see Figure 4-7) are elaborated by supervised learning algorithms, where the correspondence between the position (input) and the value of the physical quantity measured in that position (output) is exploited to infer the overall behavior of the spatial field. The main challenges arising during this process are related to the measurement noise and the fact that data are taken in random locations. In addition, in crowd mapping the Big Data issue is of crucial importance because the amount of data collected could increase exponentially with time making its memorization

and processing unaffordable. Therefore, there is the need for efficient statistical representation of the spatial field and processing algorithms with a computational complexity eventually not dependent of the number of measurements. A significant step toward this direction is represented by the theory of Gaussian process (GP), which is a powerful and widely adopted statistical tool. However, its application to the problem of spatial field estimation in the context of crowd mapping might suffer from memory and complexity issues as they typically grow fast with the number of collected measurements.

In our paper [1] we propose a combined GP-State space method whose complexity and memory requirements do not depend on the number of data measured. This allows an efficient statistical characterization of the spatial field which can be easily updated once new data become available, thus making it well-suited for crowd mapping. An experimental campaign involving a high accuracy positioning system and a magnetic mobile sensor is described and data collected are used to validate the method proposed.

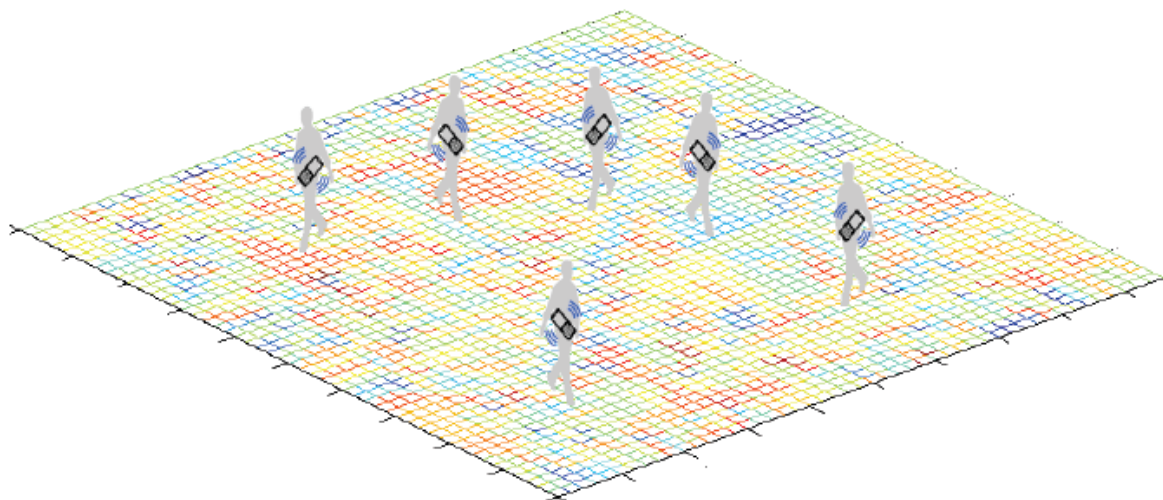


Figure 4-7 A typical crowd mapping scenario such as magnetometer and Wi-Fi interface (crowd mapping)

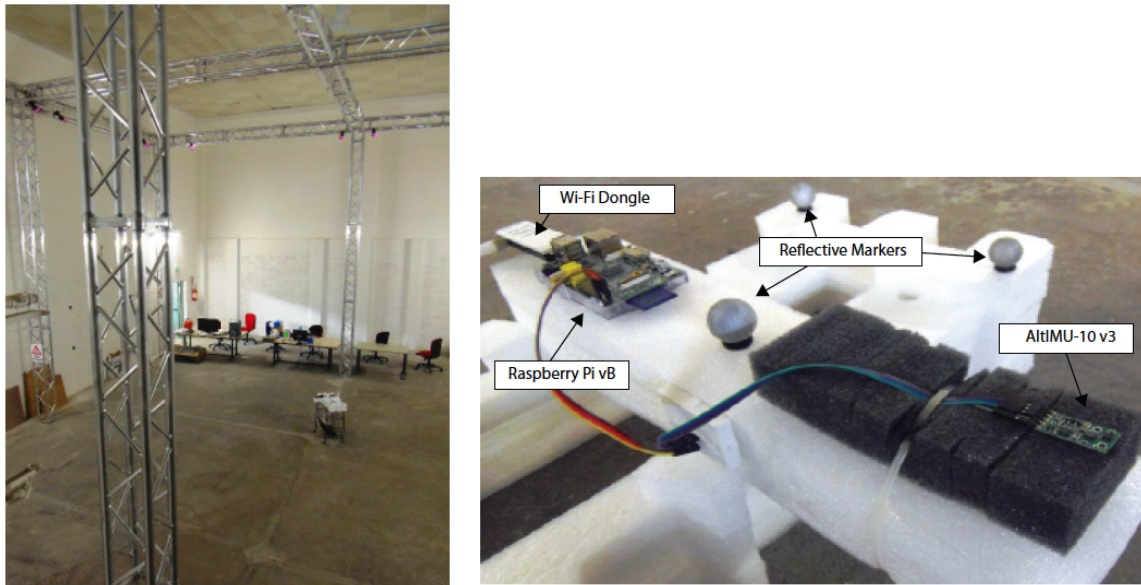


Figure 4-8 The CASY laboratory at the University of Bologna equipped with the camera-based motion tracking system and The mobile device used to collect measurements

4.1.2.2 Measurements Setup

The experimental validation has been carried out in the CASY (Center for Complex Automated Systems) flight arena at the University of Bologna, Cesena campus, shown in Figure 4-8. The laboratory is equipped with a motion tracking system composed of 22 infrared cameras (VICON Bonita 10) each one characterized by 1 Mpixel resolution. The overall system is able to localize targets within a tracking volume of $(11 \times 11 \times 11) \text{m}^3$ with less than 0.5 mm accuracy at 250 Hz. Such extremely high positioning accuracy allows to consider position errors negligible. Measurements of the geomagnetic field have been collected through an ad hoc hardware platform shown in Figure 4-8 emulating a mid range mobile smartphone. The platform is composed of a Raspberry Pi vB unit connected via I2C bus to a Pololu AltIMU-10 v3 inertial measurement unit (IMU) board, providing also geomagnetic measurements with a resolution of 0.160 mGauss and RMS noise of 5 mGauss, developed in a previous experimentation with CTTC. Data collected by the mobile platform are sent to a central unit through a standard Wi-Fi wireless link in line with the crowd sensing philosophy. The platform was continuously tracked using ad hoc markers coated with a material capable of reflecting the infrared radiation generated by the infrared cameras. To prevent excessive electromagnetic interference, the IMU board was placed far enough from the Raspberry Pi and the cables supplying the continuous current.

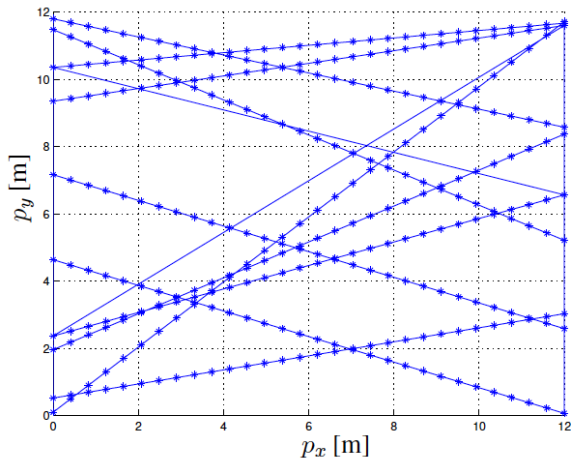


Figure 4-9 Example of random paths followed by mobile users. $N = 300$. Dots represent locations where measurements were taken.

4.1.2.3 Experimental Results

During the experimental campaign, the modulus of the geomagnetic field was measured in a dense grid of 4765 points within the monitored area. This rich set of data was utilized to provide a function very close to the original field, shown in Figure 4-10-left, used as reference for performance assessment of the GP-state space method proposed in [1]. Specifically, in each test the presence of mobile users traveling along random path and collecting a reduced amount of N measurements were emulated. In Figure 4-9 an example of such random paths is shown. In Figure 4-10-right the estimated field obtained using (8) and (10) in [1] with $B = 7^2$ and $N = 200$ is reported when perfect position knowledge is available. The corresponding root mean square error (RMSE) can be observed in Figure 4-11. As can be seen, the qualitative reconstruction fidelity is quite good. Higher values for B and N , respectively, $B = 11$ and $N = 300$, are used to derive the estimated field shown in Figure 4-12 in the form of contour plot, and in terms of RMSE. Despite the larger number N of measurements, it is evident that the reconstruction quality is worse than that in Figure 4-10. This aspect is better investigated in Table I where the RMSE is reported for different combinations of N and B . Even though the larger the number of collected measurements the better (lower RMSE values), there is an optimum value of B , i.e., the bandwidth of the GP, minimizing the RMSE corresponding to the best matching with that of the spatial field. In fact, if B is too high, the problem becomes overdetermined and a performance degradation arises. On the contrary, if B is too small, there are not enough degrees of freedom to well approximate the spatial field. As a consequence, the choice of parameter B is critical and will be object of future investigations. Previous results have been obtained assuming negligible positioning errors thanks to the extremely high-accuracy of the camera-based motion tracking system used. Now we analyze the effect of positioning errors on spatial field reconstruction. Artificial positioning errors, modeled as zero mean Gaussian RVs with standard deviation σ_p in both spatial dimensions, are added. The RMSE for different values of N and σ_p is reported in Table II when $B = 7$. As expected, the impact of positioning errors could be significant but it can be partially mitigated by increasing the number of measurements. Finally, Table III shows the joint effect of B and σ_p on the RMSE. Results indicate that small values of B lead to a lower sensitivity to positioning errors even though a bandwidth mismatch could seriously compromise the reconstruction quality.

² Parameter B is defined in [1] and it is related to the estimated spatial bandwidth of the field.

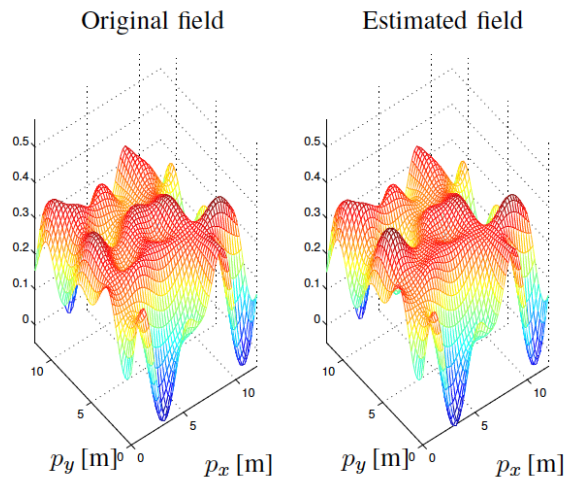


Figure 4-10 Original and estimated spatial fields [Gauss] with $N = 200$ and $B = 7$.

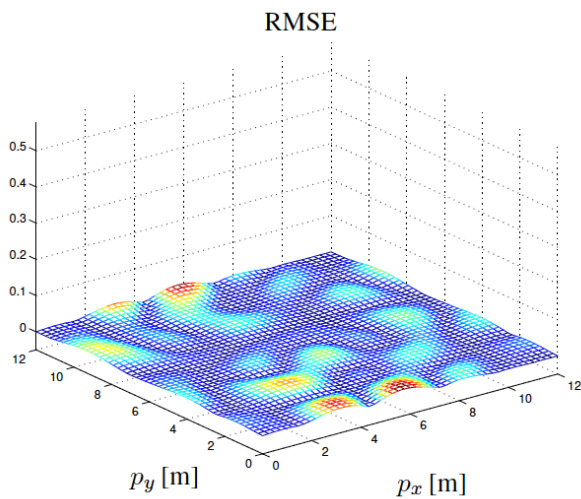


Figure 4-11 Reconstruction RMSE [Gauss] with $N = 200$ and $B = 7$.

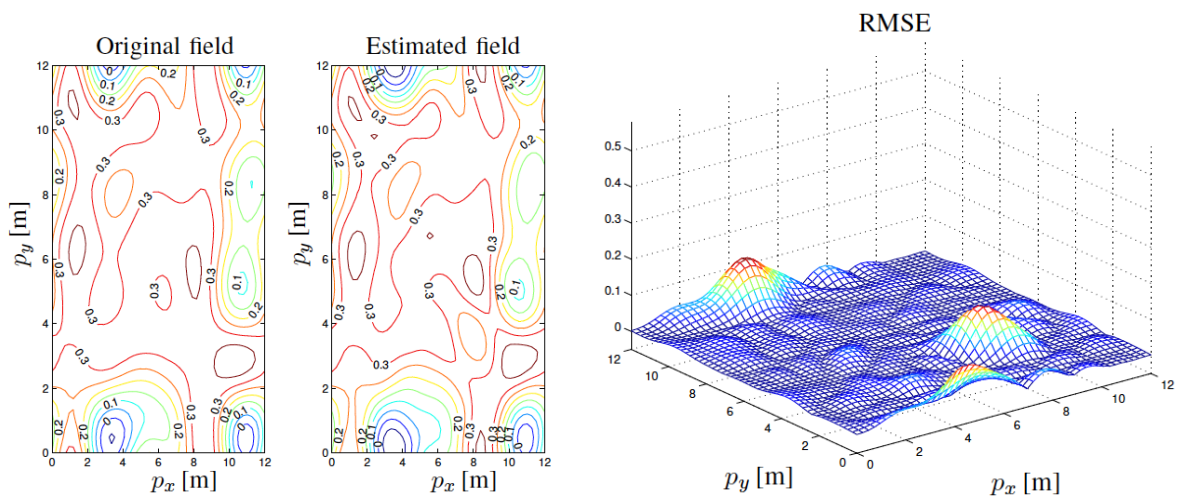


Figure 4-12 Contour plot of the original and estimated spatial fields [Gauss] with $N = 300$ and $B = 11$, and reconstruction RMSE [Gauss].

TABLE I
RMSE [GAUSS]

N/B	5	7	9	11	13
100	0.055	0.038	0.073	0.122	0.154
200	0.056	0.008	0.018	0.029	0.068
300	0.057	0.007	0.009	0.023	0.062
400	0.056	0.007	0.008	0.016	0.049
500	0.055	0.004	0.008	0.02	0.049

TABLE II
RMSE [GAUSS] - $B = 7$

N/σ_p [m]	0	0.1	0.2	0.5	1
100	0.038	0.037	0.047	0.068	0.086
300	0.007	0.028	0.039	0.053	0.067
500	0.004	0.018	0.025	0.04	0.056

TABLE III
RMSE [GAUSS] - $N = 500$

B/σ_p [m]	0	0.1	0.2	0.5	1
5	0.055	0.055	0.056	0.059	0.065
7	0.004	0.018	0.025	0.04	0.056
9	0.008	0.03	0.034	0.049	0.063
11	0.02	0.047	0.045	0.081	0.088

In conclusion, the proposed combined GP-state space method for distributed sensing of spatial fields using mobile devices allows an efficient statistical characterization of the spatial field both in terms of representation and computational complexity which is independent of the number of measurements collected. This makes the proposed solution particularly appealing for crowd mapping applications where a huge amount of data is expected to be collected in random locations. The case study reported has provided an experimental validation of the method and some useful insights on the effect of the main system parameters and position errors on the spatial field estimation accuracy.

References

[1] D. Dardari, A. Arpino, F. Guidi, and R. Naldi, "A combined GP-State space method for efficient crowd mapping," in IEEE ICC 2015 - Workshop on Advances in Network Localization and Navigation (ICC'15 - Workshop ANLN), London, United Kingdom, Jun. 2015.

4.2 Achievements of JRA#3 " Experimental activity on data sensing and fusion "

4.2.1 Evaluation of Distributed Non-Asymptotic Confidence Region Computation over Wireless Sensor Networks

4.2.1.1 Introduction

A Wireless Sensor Network (WSN) can be defined as a network of sensing devices, denoted as nodes, which can exchange the gathered information through wireless links. Nodes are usually low cost, small size and energy-limited sensing devices that collaborate to perform a common task, such as the monitoring of an environmental parameter. They can be stationary or mobile and are usually organized into a network. A centralized approach, in which a central unit collect all the information, or a distributed approach, where all nodes accomplish the objective task, can be adopted, depending on the application requirements. In general, the scarce robustness to central unit failures and poor network scalability make distributed approaches more desirable.

Depending on the task of the WSN, a confidence region associated to the estimate of the monitored parameter may be more informative than a point estimate without a measure of its uncertainty. Classical Cramer-Rao-like bounds or Kalman filtering are usually adopted to derive the estimation accuracy. However, strong assumptions on the measurement noise are required and a good characterization of confidence regions is only possible for a large number of measurements.

On the contrary, the Sign Perturbed Sums (SPS) [1] method allows a central unit to derive a confidence region from a finite set of measurements (non-asymptotic confidence region). In [2] a distributed version of SPS has been investigated and a novel information diffusion strategy, named tagged and aggregated sums (TAS), was presented and compared to other information diffusion strategies in terms of amount of information exchanged among nodes.

In [2], in particular, the amount of exchanged data is derived, analytically and via simulations, for different information diffusion strategies and network topologies.

Hereafter we experimentally investigate the performance of the same information diffusion algorithms using off-the-shelf sensor nodes in an actual environment.

4.2.1.2 Modified Flooding (FL) and Tagged and Aggregated Sums (TAS) algorithms

This section briefly describes the information diffusion strategies we considered to implement the SPS algorithm.

-Modified Flooding

The plain flooding algorithm is a simple information diffusion strategy in which each node broadcasts its measurements along with those of the other nodes that it has received in the meanwhile. This strategy is very simple but not very efficient.

A more efficient version of the flooding strategy can be obtained by sending each information only once. This is done by the "modified flooding" algorithm, which generates in each node a table containing the information already transmitted. Figure 4-13 shows an example of the "modified flooding" behavior: In the beginning node $j=1$ knows only its data; in the first transmission round it broadcasts its information and keeps trace that this information has been already transmitted (green arrow). Then, it receives information related to nodes $j=5$ and $j=9$ and the table is updated. In the following transmission round, the node checks the table and transmits only the new information, related to nodes 5 and 9, marking that now the last transmitted information is the one related to node 9 (green arrow).

Indeed, actual implementations of the flooding strategy usually behave as the "modified flooding" strategy, hence in the following we will consider the "modified flooding" strategy and we will denote it with the abbreviation FL.

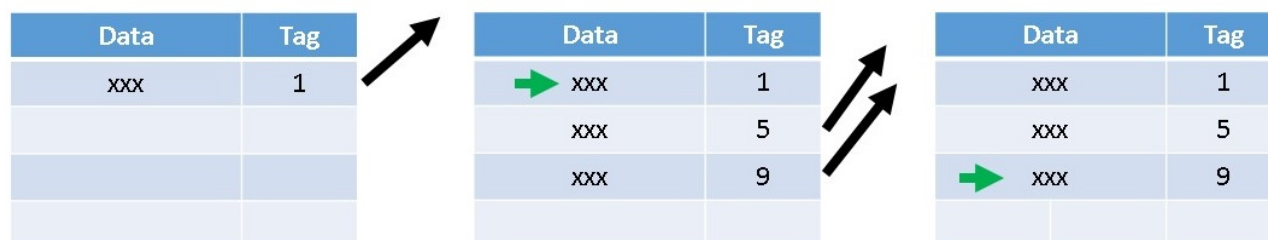


Figure 4-13: Example of information table of a node $j=1$ when FL is used as information diffusion algorithm.

-TAS algorithm

The TAS algorithm consists of six phases, which are detailed in [2]. The main idea of the TAS strategy is to directly propagate the partial sums needed to perform the SPS algorithm, instead of transmitting each single value. Along with the partial sum, a tag vector must be also transmitted in order to keep trace of the nodes contributing to the partial sum. The tag is, in particular, a binary vector with a number of bits equal to the number of nodes. As an example, if node $j=1$ receives the partial sum of the information related to node $j=2$ and node $j=5$, the correspondent tag must have the second and the fifth bits set to “1”. Then, a generic node j that receives the aggregated information (that is, the partial sum) is aware of which nodes contributed to the partial sum and decides whether there is a new contribution or not. The example previously presented for the FL algorithm is shown again in Figure 4-14. **Errore. L'origine riferimento non è stata trovata.** for the TAS algorithm. At the first round, node $j=1$ broadcasts its own information and marks the correspondent line in the table as “already transmitted”. Then, it receives information related nodes $j=5$ and $j=9$, and the table is updated. In the following transmission round the node checks the table and aggregates, in a partial sum, only the new data. The sum is then broadcasted and both the new rows of the table are marked as “already transmitted”. Through this simple example, it is easy to understand that the TAS algorithm works in a more efficient way respect to the FL algorithm.

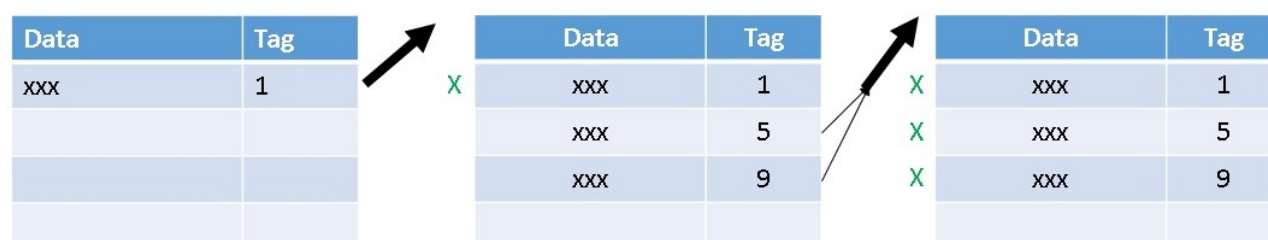


Figure 4-14: Example of information table of node $j=1$ when TAS is used as information diffusion algorithm.

4.2.1.3 Devices characterization

Embit sensor nodes EMB-Z2530PA were used to investigate the performance of the above-described algorithms in actual scenarios. EMB-Z2530PA incorporates a temperature sensor, an IEEE 802.15.4\ZigBee communication device and a Texas Instruments CC2530 microcontroller (with 8 Kbyte of RAM and 256 Kbyte Flash memory) that controls all operations. It combines high performance, small dimensions and low cost. The block diagram of the EMB-Z2530PA is shown in Figure 4-15 [4].

The RF front end includes a power amplifier that allows an output power up to 20 dBm. Along with the low noise amplifier of the receiving section, that allows a sensitivity of -105 dBm, it provides a coverage distance up to 500 meters in line of sight.

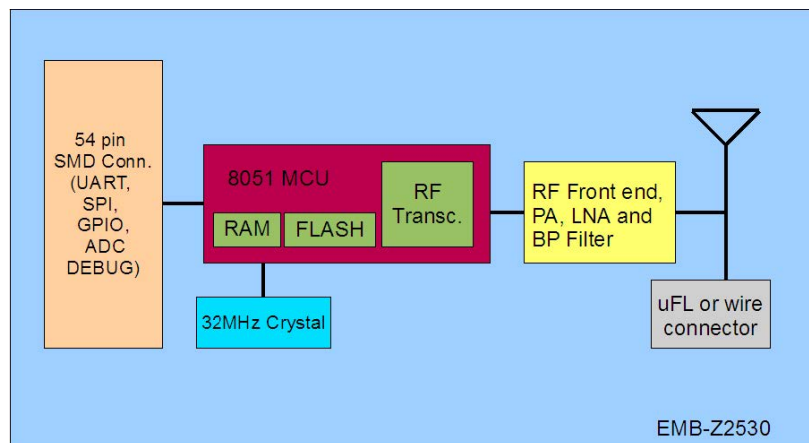


Figure 4-15: Block diagram for the EMB-Z2530PA.

The radio module is controlled by the RF core, which is composed by a modulator, a demodulator, a finite state machine (that controls the transceiver state and most of the dynamically controlled analog signals), an automatic gain control (to adjust the gain of the low noise amplifier), a frame filtering and source matching, a frequency synthesizer (that generates the carrier signal), a command strobe processor (that process all command issued by the CPU), and a RAM memory. According to the IEEE 802.15.4 standard, carrier frequencies from 2394 MHz to 2507 MHz are supported. IEEE 802.15.4 specifies 16 channels, 5 MHz apart, within the 2.4 GHz band, numbered from 11 to 26. The center frequency of a channel is given by [5]:

$$f_c = 2405 + 5 (k - 11) \text{ MHz}$$

$$K = 11 \dots 26.$$

The modulated signal is an offset-quadrature phase shift keying (O-QPSK) with half-sine chip shaping, in which each chip is shaped as a half-sine, transmitted alternately in phase and in quadrature channels with one-half chip period offset. The transmission register can hold 128 bytes.

The CSMA/CA protocol is used to share the access to the medium. A node listens to the channel before transmission to determine whether someone else is transmitting or not. If the channel is idle the node can transmits, otherwise a back-off algorithm starts. The back-off time is randomly chosen in a range between zero and $W-1$, where W is the contention window length. After each unsuccessful transmission the back-off windows size is doubled up to a maximum value; once the back-off window size reaches its maximum value it will stay at that value until it is reset after a given number of transmission attempts.

The Embit devices are easily programmable through the CC debugger provided by Texas Instruments (Figure 4-16). They can be used in many applications, such as building automation, metering, industrial automation and healthcare.



Figure 4-16: Representation EMB-Z2530PA sensor with debugger.

4.2.1.4 Data packets

Figure 4-17 shows the schematic view of IEEE 802.15.4 frame format. The synchronization header (SHR) consists of a preamble sequence followed by the start of frame delimiter (SFD), while the PHY header consist only of the frame length field. The frame control field, data sequence number and address information follow the frame length field, while at the end of the MPDU the frame check sequence is calculated over the MPDU following a polynomial definition. The transmission register can hold 128 bytes and, as we can see in Figure 4-17, considering that the 16 bytes address information, the maximum achievable payload is 102 bytes. Temperature measurements are carried out in our experimental setup in order to consider a real application. The measured value is represented with 2 bytes.

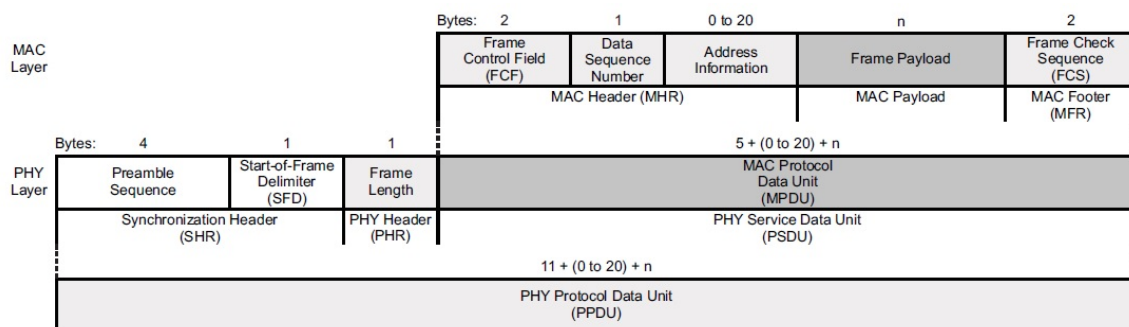


Figure 4-17: Schematic view of the IEEE 802.15.4 frame format.

-FL data packet

The modified flooding algorithm generates at runtime a table of information available at each node; an information already transmitted by a node is never transmitted again by the same node. The data are stored with their respective tags, that represent the correspondent source node. The tag length depends on the number of sensors within the network (with a byte is possible to have up to 255 sensors). During a transmission round, the new data with the relative tags are transmitted, so at each round the number of transmitted bytes is:

$$number_{Txbytes_{FL}} = number_{newinformations} * (2 + number_{tagbytes_{FL}}).$$

-TAS data packet

The TAS aggregates the information to reduce the number of transmitted bytes. Also the TAS algorithm creates at runtime a table of information available at each node and an information already transmitted by a node is never transmitted again by the same node. At each transmission round, the TAS algorithm derives a partial sum with the new information contained in the table. Differently from the FL algorithm, the tag is created by setting a "1" in the position corresponding to the sensor's index; with a byte is thus possible to cover up to 8 sensors. At each round the number of transmitted bytes is:

$$number_{Txbytes_{TAS}} = 2 + number_{tagbyte_{TAS}}.$$

4.2.1.5 Implementation of the algorithms

This paragraph describes the practical implementation of the FL and TAS information diffusion algorithms. In both cases, a network coordinator is present. At the beginning, the coordinator sends a start message, that triggers the execution of the information diffusion algorithm in each node. In unstructured topologies, after the reception of the start message, each node measures the temperature and broadcasts the information. In structured topologies, instead, the tree network must be established before starting the algorithm. Starting from the device that acts as the root, each sensor search for a random number of children, so that is possible to create different trees at each run. Packets will be exchanged beginning from the last level up to first level and then in the opposite direction. Once a father transmits the information of its children to its father, also its children receive the information. At the end, regardless of the type of topologies, the coordinator forwards an end message to stop the execution of the information diffusion algorithm and collects the data to derive the performance metrics.

- FL algorithm

After the reception of the start message, each node measures the temperature and broadcasts the information. At each received packet, the correspondent information content is evaluated. If a new information is available, it is stored in the node's table, otherwise it is discarded. After the reception phase, the transmission phase starts: each device check its table and if new data are present, they are appended to the packet to be sent. When the entire table has been scanned, the packet is finally transmitted (provided that the payload is not empty). At the end of the execution of the algorithm, the coordinator collects the amount of bytes transmitted/received by each node.

- TAS algorithm

After the reception of the start message, each sensor measures the temperature and start transmitting and receiving data. Packets will be exchanged beginning from the last level up to first level and then in the opposite direction. Once a father transmits the information of its children to its father, also its children receive the information.

Each sensor inspects the tag of each new received packet to understand if the partial sum contains new contributions. If new data are present, summed with already known ones, the new data are distilled and stored. After the reception phase, the transmission phase starts: each node checks its table and if new information are present, they are used to derive a new partial sum, which is transmitted when the table has been completely scanned. At the end of the execution of the information diffusion algorithm, the coordinator collects the amount of bytes transmitted/received by each node.

4.2.1.6 Preliminary results

In this paragraph we evaluate the performance of the FL and TAS algorithms in a simple networks with 15 or 20 nodes. We considered a flat or a tree network topology.

Setting the same transmission time to each sensor

In the first trial, the same transmission time was set in each sensor to investigate what happens if all sensors try to transmit at the same time in a small area.

- Flat topology

We set up a network, formed by N sensor nodes, structured on a single level of hierarchy. The network is fully connected so that each node can directly communicates with the others. One of these acts as a coordinator, that starts the information diffusion algorithm (either FL or TAS) and, at the end, collects the amount of packets transmitted/received by all nodes (Figure 4-18). In particular, the coordinator/collector sends a “start” packet to trigger either the TAS or the FL algorithm in each sensor for a finite number of rounds N_{round} . In the first round each sensor measures and transmits its data, whereas during the other rounds the sensors receive the information from the other nodes and execute the proper information diffusion algorithm (TAS or FL) before transmitting the next packet.

As a first step, we evaluated the impact of the back-off algorithm with $N_{round} = 10$.

The behavior of the back-off algorithm has been controlled changing the maximum number of transmission retries, that ranges between 0 and 5, the initial length of the contention window $W_{min} = 2^{minBE}$, with minBE in $[0, maxBE]$, and the maximum contention window size $W_{max} = 2^{maxBE}$ with maxBE in $[3, 8]$.

At the completion of the N_{round} rounds, the total amount of data transmitted/received by each node is counted and transmitted to the collector. The procedure is repeated hundred times in order to derive the average metrics.

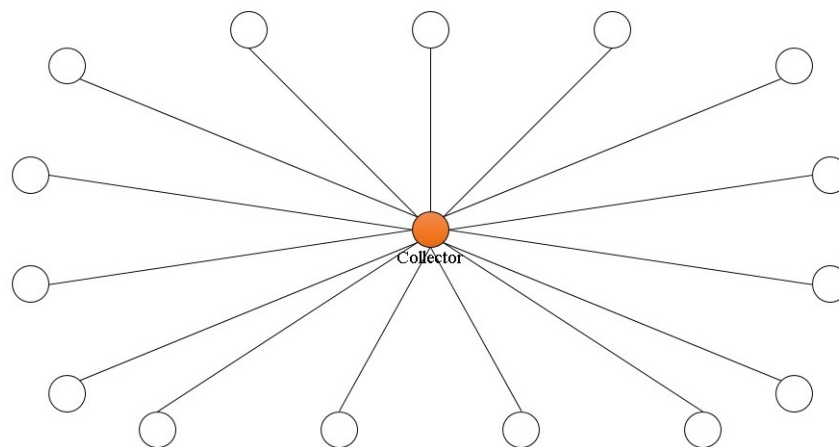


Figure 4-18: Representation of a random structured network.

Figure 4-19 shows the percentage of information received by the nodes varying the back-off parameters with the FL algorithm. We set the maximum number of transmission retries equal to 5; minBE= 0, 3 or 4, and maxBE=8. As we can see, collisions highly affect the algorithm performance. In fact, even in the case with maximum number of transmission retries=5, minBE=4 and maxBE=8, only the 22% of the sensors received all data from their neighbors, thus showing that collisions are still significant.

To further investigate this phenomenon, we derived the FL performance as a function of N , in the same condition previously assumed. As can be observed in Figure 4-20, the FL algorithm works perfectly when $N < 8$, then number of collisions increases, deeply affecting the system performance. For larger values of N the amount of lost packet increases significantly.

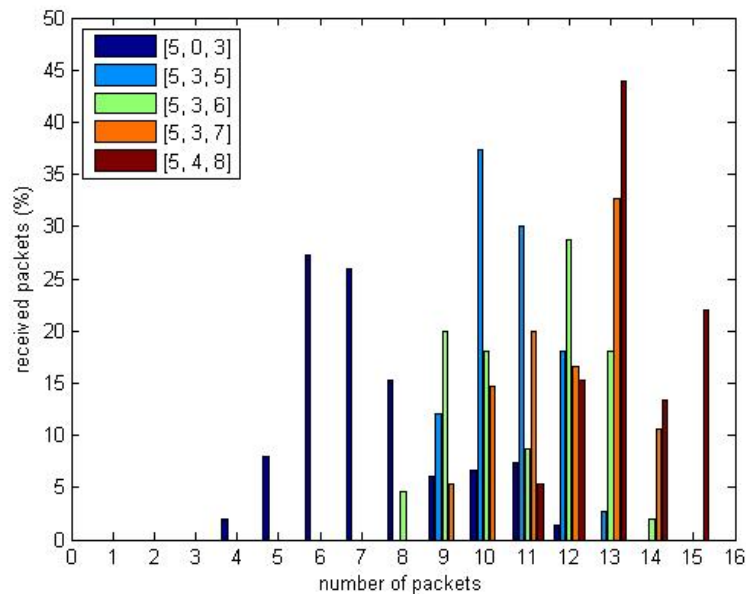


Figure 4-19: Percentage of information packets received. Experimental results of FL algorithm in unstructured topology of 15 nodes, varying the back-off parameters.

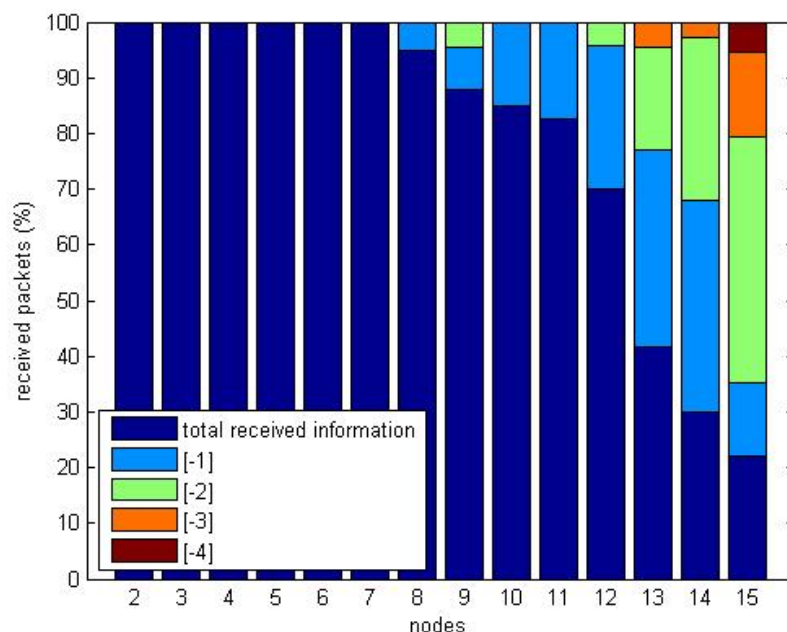


Figure 4-20: Percentage of received information packets. Experimental results of FL algorithm in unstructured topology varying the number of devices.

- Tree topology

We considered a tree topology with $N=20$ nodes, where each node has a number of sons defined a priori, in order to have a preliminary insight on the algorithms performance in a controlled situation.

During the initialization phase the nodes connect each other according to the a-priori defined tree structure. Only at this point the information diffusion algorithm is started. The information is broadcast by each node but only the right father retains it (packet filtering). We choose $N_{round} = 10$, although 2 or 3 rounds are enough to complete the information exchange in the case of trees with 3 or 4 levels, as the ones we considered. At each round, the nodes send their information to their father, until the information will reach the coordinator at level one.

Figure 4-21 shows four different trees with three levels, while Figure 4-22 **Errore. L'origine riferimento non è stata trovata.** shows four different trees with four levels. Sensors are represent with circles and the number written inside represents the sensor's index. The percentage written near each sensor indicates the percentage of information received with respect to the maximum amount of information that each sensor should receive, considering that the information collected by the root is not sent back from the collector to the last level.

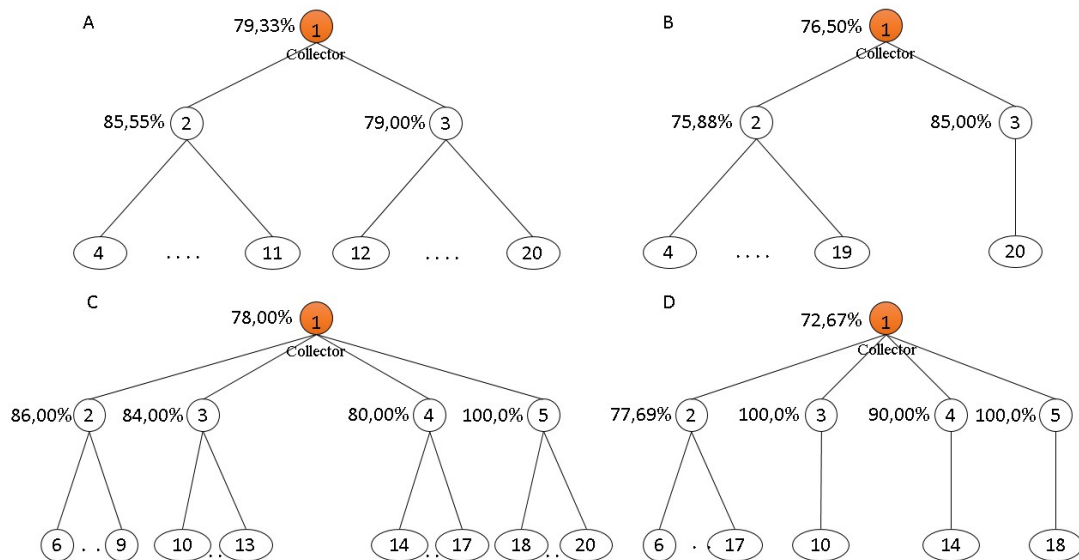


Figure 4-21: Example of experimental results over tree topologies with three levels using FL algorithm.

Also in this case the packet collisions impacts on the performance of the FL algorithm but the hierarchical network structure allows to reduce the number of simultaneous transmissions with respect to the flat topology.

Figure 4-23 **Errore. L'origine riferimento non è stata trovata.** and Figure 4-24 show similar results for the TAS algorithm. As we can see, with TAS the amount of lost data is generally larger with respect to FL. This is due to the fact that a packet loss with TAS is more critical than with FL in terms of amount of lost data.

Setting different transmission times for each sensor

In the second trial, the transmission times were different in each sensor, in order to consider a realistic implementation in which sensors are not synchronized. Flat and tree topologies are considered to evaluate the impact of the MAC protocol. The algorithms were performed 100 times with 10 rounds each time. As for the MAC parameters, the maximum number of retries is equal to 5, minBE is equal to 3 and maxBE is equal to 5.

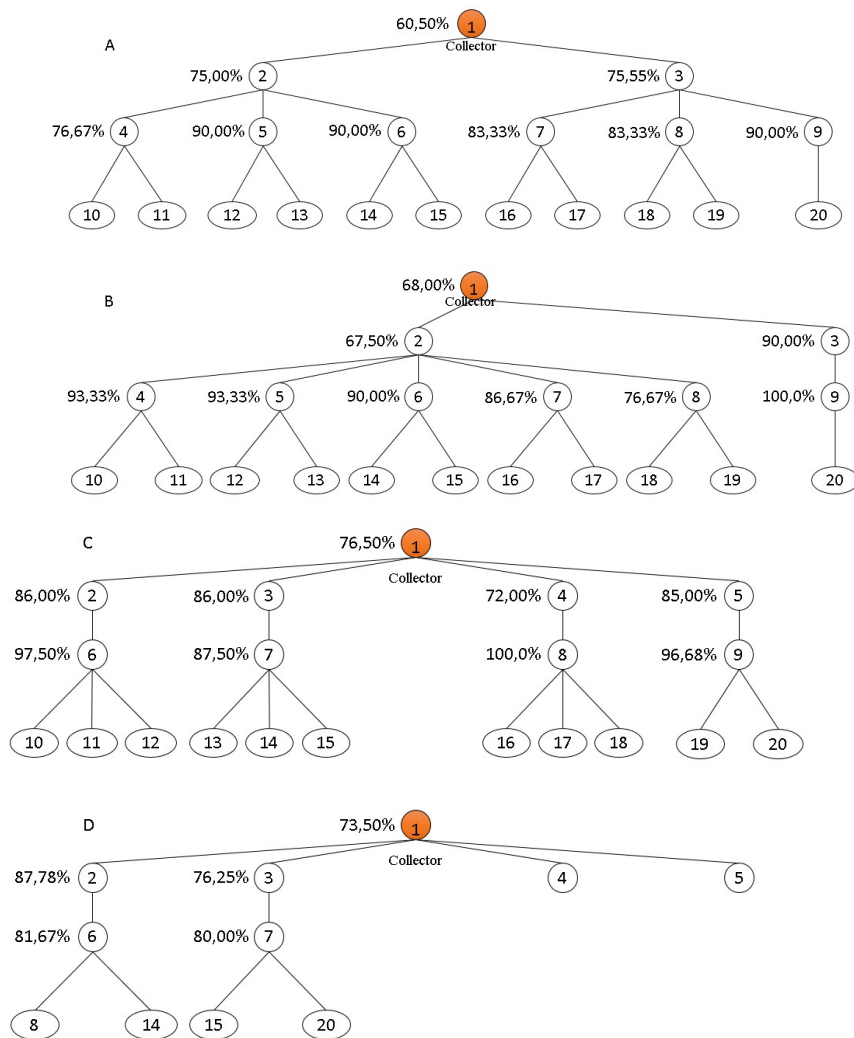


Figure 4-22: Experimental results over tree topologies with four levels using FL algorithm.

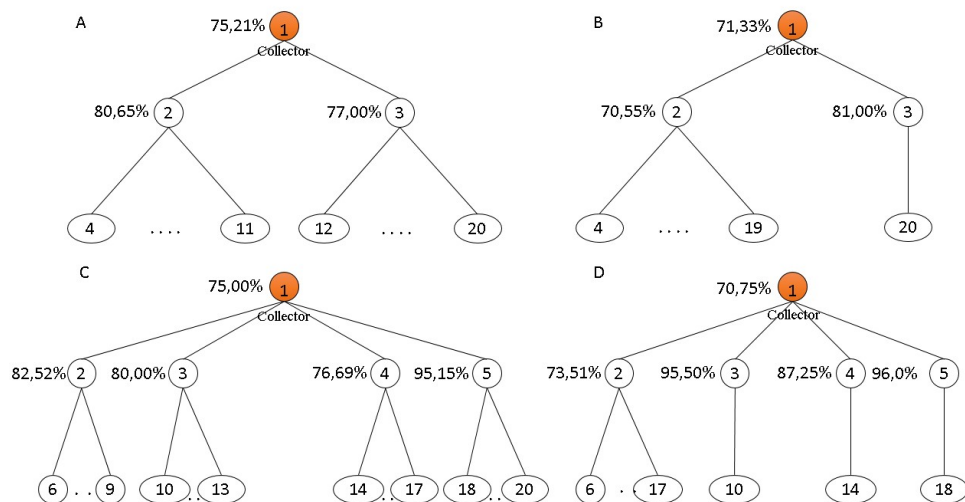


Figure 4-23: Experimental results over tree topologies with three levels using TAS algorithm.

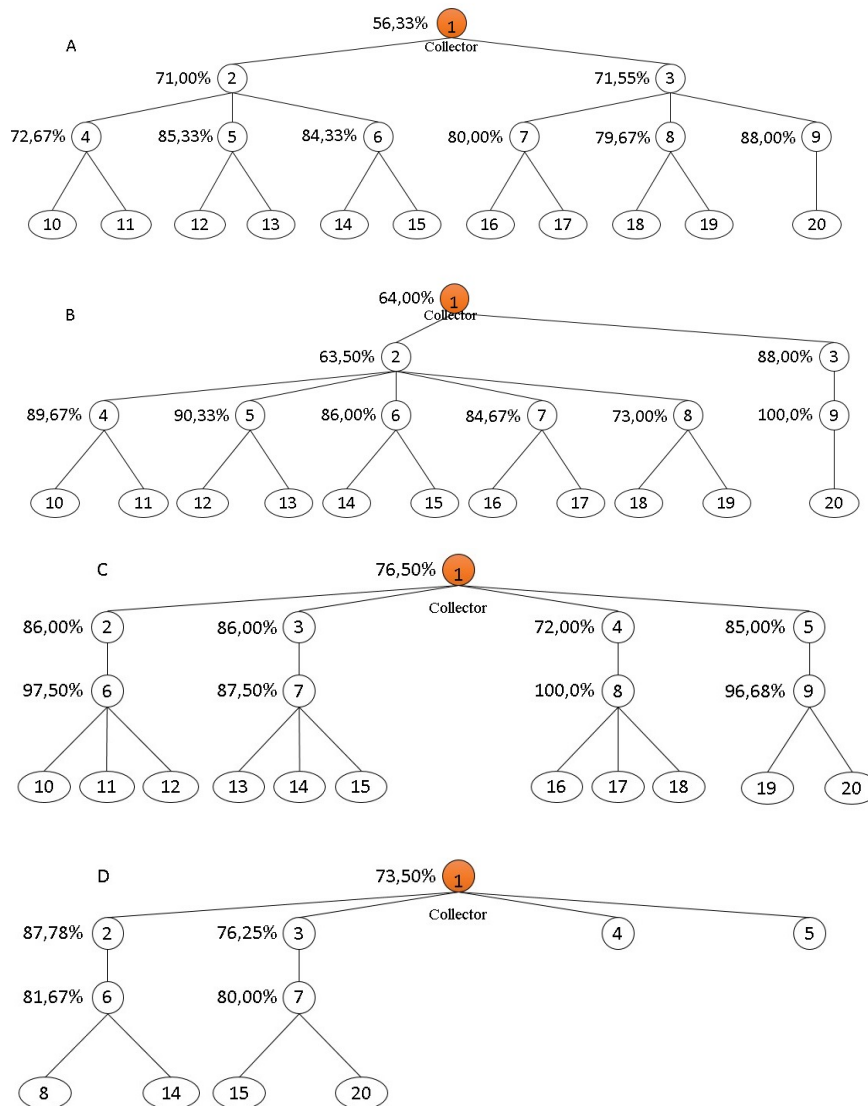


Figure 4-24: Experimental results over tree topologies with four levels using TAS algorithm.

- Flat topology

We considered a network formed by $N=15$ sensor nodes, structured on a single level of hierarchy (Figure 4-18). The network is fully connected, so that each node can directly communicate with the others. One of these acts as a coordinator. To investigate if something changes respect to the previous trial, we derived the FL performance varying the duration of rounds. As can be observed in Figure 4-25, **Errore. L'origine riferimento non è stata trovata.** the FL algorithm works perfectly even with 15 nodes as far as the duration of a round T_{round} is greater than 0.5 seconds.

- Tree topology

We considered a random tree topology, where each node has a number of sons that can vary. The number of nodes forming the network is $N=20$. A different random tree is realized at each run. The information is broadcast by each node but only the right father will retain it. The information is exchanged starting from the lowest level up to the first and then forwarded inversely to the lowest levels in order to reach all the nodes.

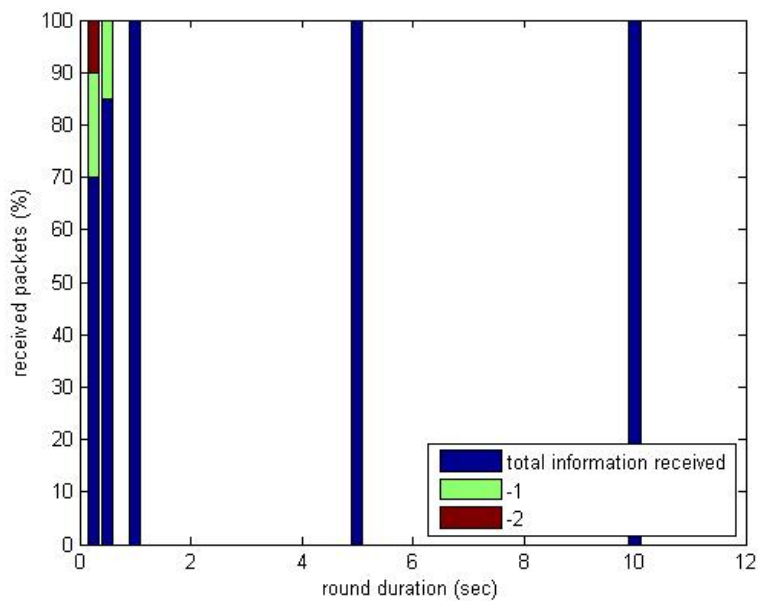


Figure 4-25: Percentage of received information as a function of round duration.
Experimental results of FL algorithm in unstructured topology varying the round duration.

Figure 4-26 shows the cumulative distribution function of the amount of transmitted data derived with the experimental setup previously described. Result are shown with a round duration of 0.25 and 1 second.

Please observe that in the case of FL the total amount of data that each sensor should transmit is 1174 bytes, whereas each node implementing the TAS should transmit 1550 bytes.

Figure 4-26 clearly shows how much the MAC layer affects the algorithms performance. Results with 0.25 seconds of duration are smaller than the other because not all the information related to the other sensor has been received and then transmitted.

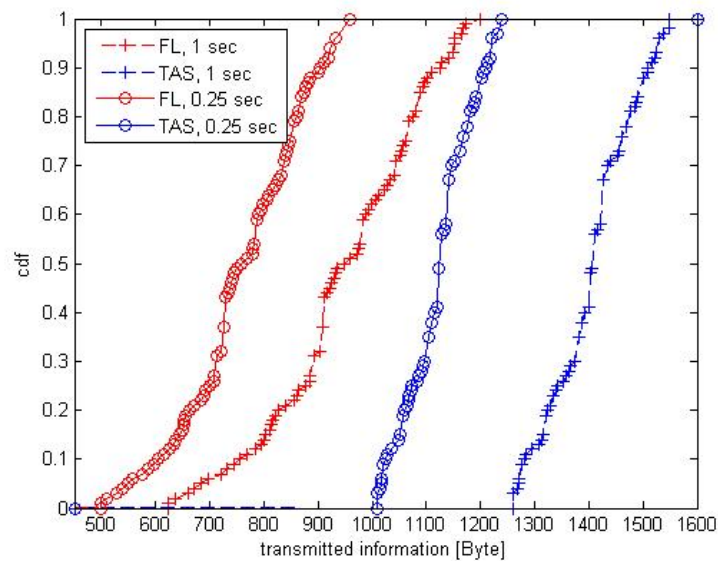


Figure 4-26: Cumulative distribution function versus the number of transmitted information. Comparison of the experimental results of FL and TAS algorithm in different trees of 20 nodes with a round time equal to 1 and 0.25 seconds.

4.2.1.7 Results

The performances of FL and TAS algorithms have been also tested in a complex actual scenario. In particular, 52 nodes were placed in a $29.50 \times 9\text{m}^2$ small office area with furniture at the WiLab laboratory (Figure 4-27). Differently from the previous cases, in which all sensors can reach each other, the communication range has been changed (properly setting the transmission power), in order to have a coverage in the order of 3 meters (low power) and 5 meters (high power). Adjacent nodes in the horizontal and vertical directions were placed at a distance of 2 m. The coordinator, working with the maximum allowable transmission power (20 dBm) in order to reach all the sensors, was placed in a central position. In Figure 4-27 the scenario layout is depicted, with the coordinator represented by an orange circle and the sensor nodes represented by blue circles.

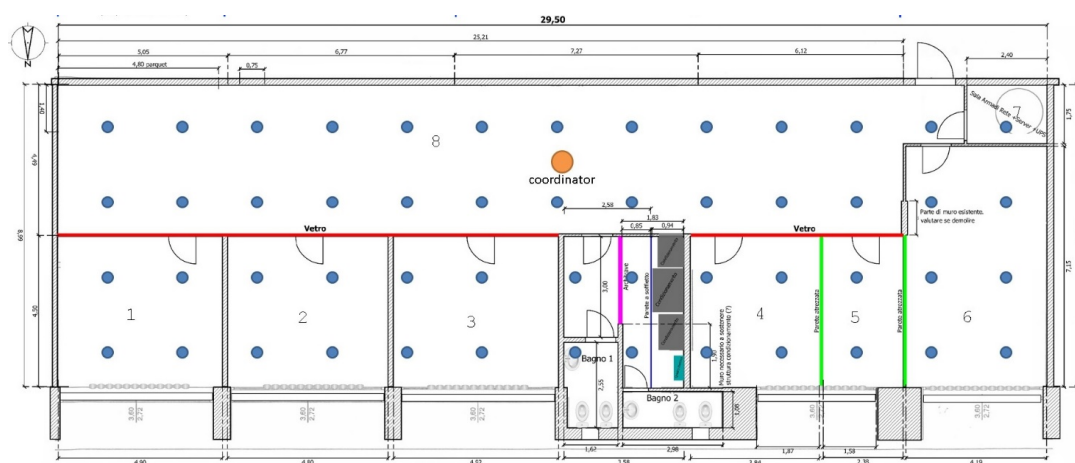


Figure 4-27: Sensors' positions at the WiLab laboratory.

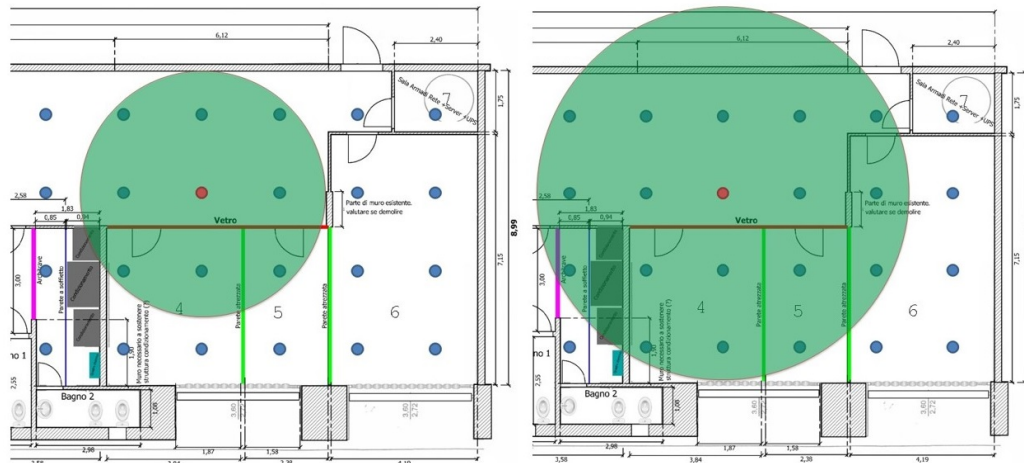


Figure 4-28: Impact of transmission range on the number of neighbors.

In the first test, an unstructured network has been considered, with $N_{round} = 20$ and $T_{round} = 1$ s. The performance of both FL and TAS have been evaluated in both cases of low and high power conditions. Of course, different transmission ranges change the number of neighbors of each node and impact on the measured performance. Figure 4-28 **Errore. L'origine riferimento non è stata trovata.** shows that with a transmission range in the order of 3 meters the number of neighbors is 8, in average, whereas this values increases to 17 with a coverage range in the order of 5 meters.

Figure 4-29 shows the cumulative distribution function of the amount of information transmitted by FL and TAS. Here we can observe that in an unstructured network the FL algorithms transmits less data than TAS.

Figure 4-30 shows, instead, the impact both the round duration and the coverage on the percentage of received information. As we can see, a reduction of the round duration leads to reduction of the amount of received information. As expected, the small coverage case provides better performance, owing to the reduced number of neighbors and, therefore, of collisions.

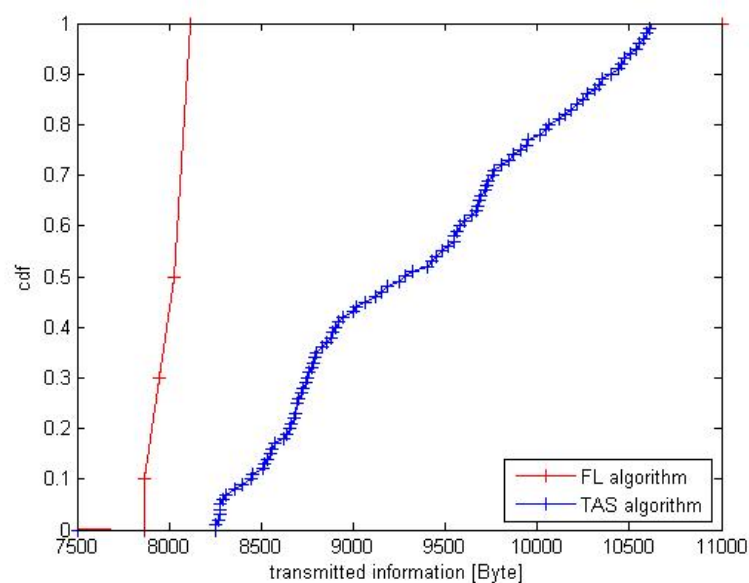


Figure 4-29: Cumulative distribution function versus the total information transmitted from all the sensors. Experimental results in unstructured topology varying the transmission power and round duration.

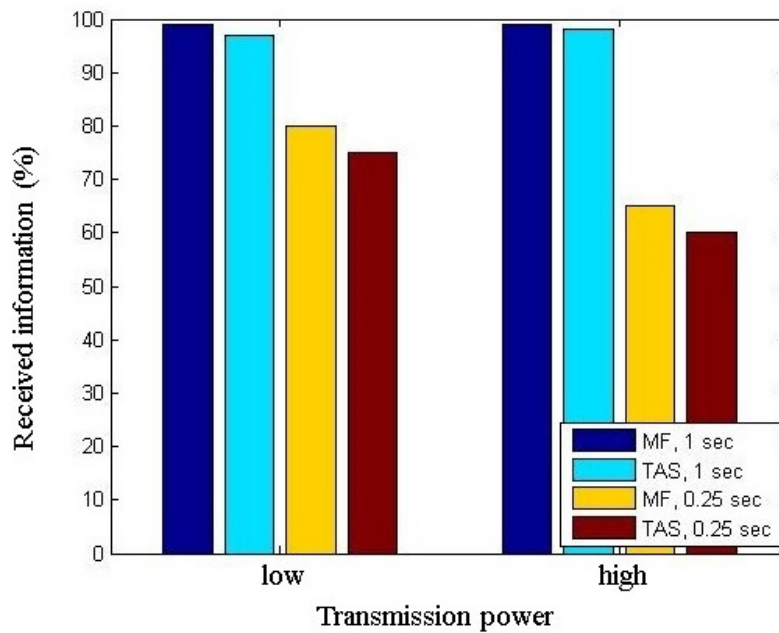


Figure 4-30: Experimental results of the average percentage of information received as a function of transmission range setting the duration of rounds at 1 and 0.25 seconds.

The random tree topology has been also investigated, considering a random number of children for each sensor. We considered $N_{round} = 20$ and $T_{round} = 1$. Simulation result obtained with this scenario are shown in

Figure 4-31 **Errore. L'origine riferimento non è stata trovata.** and Figure 4-32. In particular, the average amount of transmitted information needed to evaluate the 90% confidence region in random trees with 52 nodes is investigated in

Figure 4-31 **Errore. L'origine riferimento non è stata trovata.** Figure 4-32 shows, instead, the percentage of cases for which TAS performs better than FL (in terms of amount of transmitted information) for different values of n_p , that represents the number of parameter to be estimated. As can be seen, with $n_p=1$ TAS performs always better than FL as soon as the number of nodes exceeds 40.

Figure 4-33 shows the cumulative distribution function of the transmitted information for the FL and TAS algorithms over different trees of 52 nodes, varying the coverage and the round duration. In the case $T_{round} = 1$ s, only results with low transmission power are shown because the results with high transmission power are the same.

This figure shows how the MAC layer affects the performance. In the case $T_{round} = 0.25$ s, the amount of collisions is relevant, and the average number of packets transmitted is smaller than the case $T_{round} = 1$ s.

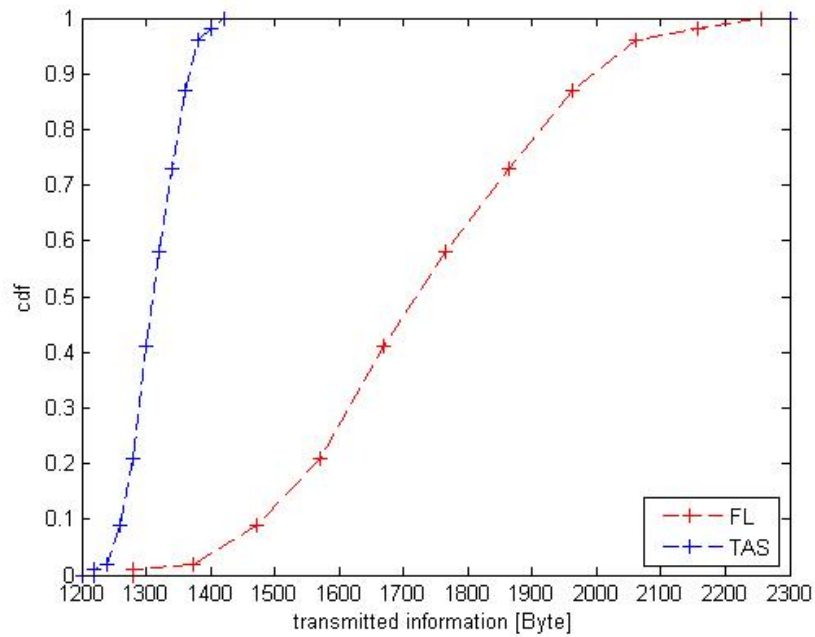


Figure 4-31: Cumulative distribution function vs the average amount of transmitted information needed for the evaluation of the 90% confidence region. N=52.

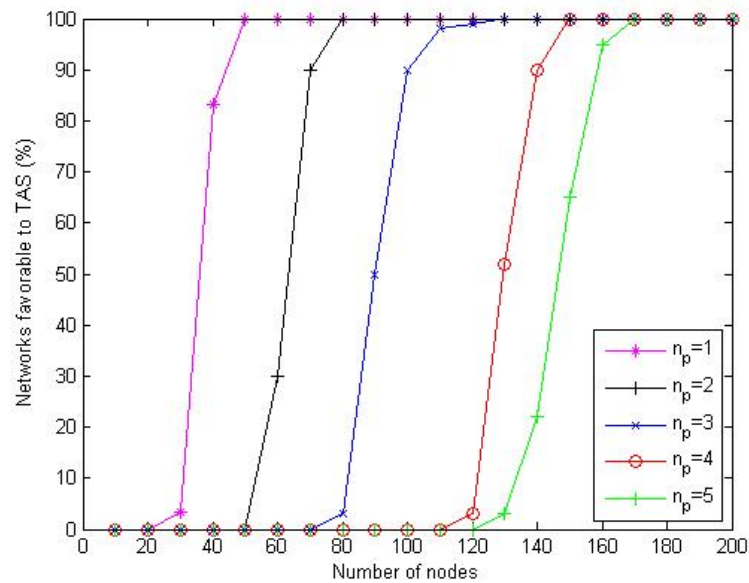


Figure 4-32: Percentage of networks favorable to TAS compared to FL as a function of the number of nodes that compose the networks. Simulation results with one- and multi-dimensional measurement.

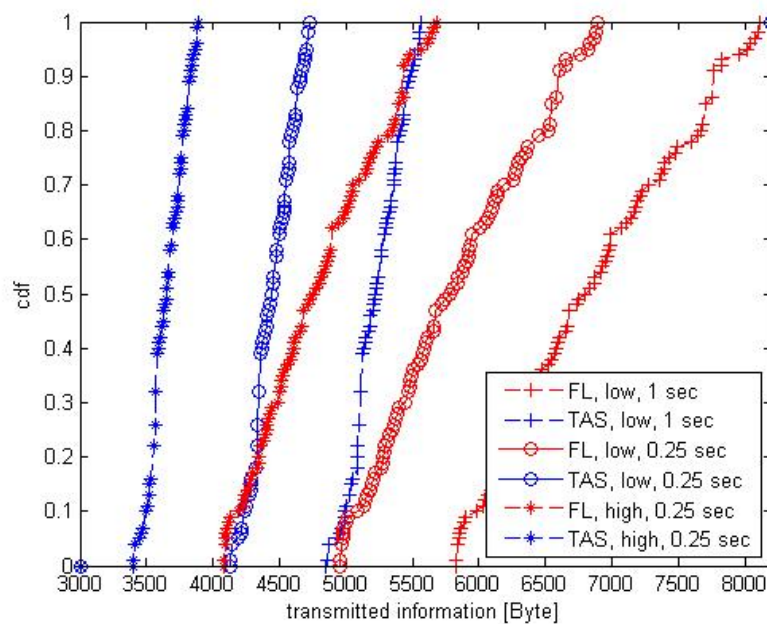


Figure 4-33: Cumulative distribution function versus the total information transmitted from all the sensors. Experimental results in tree topology varying the transmission power and round duration.

4.2.1.8 Conclusion

In this section we experimentally investigated the performance of a novel information diffusion strategy, dubbed TAS, specially designed for the distributed evaluation of non-asymptotic confidence region in WSNs with the SPS algorithm.

The TAS strategy has been compared with the classic flooding strategy in terms of transmitted/received information in an actual scenario. Both algorithms have been implemented on of-the-shelf sensor nodes that realized structured and unstructured WSNs. The impact of the MAC strategy, as well as of the network topology and transmission coverage have been highlighted and discussed.

References

- [1] B. C. Csaji, M. C. Campi, and E. Weyer, "Non-asymptotic confidence regions for the least-squares estimate," in 'Proc. IFAC SYSID, Brussels, Belgium, 2012, pp. 227–232.
- [2] V. Zambianchi, M. Kieffer, F. Bassi, G. Pasolini and D. Dardari, "Distributed SPS algorithms for non-asymptotic confidence region evaluation," 2014 European Conference on Networks and Communications (EuCNC), June 2014.
- [3] "User's guide: CC253x System-on-Chip Solution for 2.4-GHz IEEE 802.15.4 and ZigBee® Applications," Texas Instruments, pp. 1-354, Apr. 2014.
- [4] "EMB-Z2530PA datasheet," embit, pp. 1-24.
- [5] "IEEE Standard for Local and metropolitan area networks - Low-Rate Wireless Personal Area Networks (LR-WPANs)," IEEE Std 802.15.4-201, pp. 1-334, Jun 2011.

4.2.2 Experimental verification of distributed fault detection for wireless sensor network

4.2.2.1 Introduction

In wireless sensor networks (WSN), it is very important to identify and isolate nodes with defective sensors, i.e., producing measurement outliers. Recently, a distributed outlier detection (DOD) algorithm for large WSNs has been proposed in [1]. It allows each node to determine the status of its own sensor. Different from the classical solutions, the local outlier detection test (LODT) in our approach is simple, works with few measurements, but is only able to detect the presence of outliers within a set of measurement. The proposed DOD algorithm has low complexity, low communication cost, and good performance in terms of non-detection rate (NDR) and false alarm rate (FAR). Nevertheless, the results presented in [1] assume perfect communications and neglect collisions and losses.

Thanks to the experimental facilities available within EuWIn@CNIT/Bologna, this work considers the implementation of the DOD algorithm on the Data Sensing and Processing Testbed (DataSens), which consists of 100 wireless sensor nodes of type EMB-2530PA. The impact of the protocol stack and of real propagation conditions is investigated. The obtained results allow us to refine our DOD algorithm in presence of packet collisions.

4.2.2.2 Main results

In a first set of experiments, all the nodes are closely located and can receive packets from all other nodes. However, each node is assigned a random virtual location to create its set of neighbors. An interesting problem is to compare the performance of algorithm (in terms of the non-detection rate (NDR) and the false alarm rate (FAR)) with different number of initial round K_1 and final round K_2 as a function of total execution time T_e . The result is presented in Figure 4-34(a), where different number of defective sensor nodes N_d are also considered. Independent experiments have been repeated 1000 times for all the cases. As expected, less packet collision occurs as T_e increases and thus the performance of the algorithm becomes better. In both cases where $N_d = 1$ and $N_d = 3$, both NDR and FAR become smaller as the number of initial rounds K_1 increases, considering the same T_e .

In a second set of experiments, the DOD tests are performed in a more realistic situation where the network is not fully connected. The network topology is shown in Figure 4-35, where 41 nodes are randomly deployed over the right side of WiLab. The position of nodes remains unchanged, each node has a given probability to be defective in each test. In our tests, the defective probability is set to be 15%, the DOD is performed with $K_1 = 5$ and $K_2 = 1$. Figure 4-34(b) illustrates the average performance of DOD in different areas and using different transmission power (TxP). The results show that the nodes in the center have lower NDR and FAR than those at sides, considering the same TxP. As the testbed has a limited space, the performance of DOD suffers from boundary affects. Three different TxP are considered with their values $P_1 > P_2 > P_3$. Comparing the average NDR and FAR of the nodes in the center, the results highlight that NDR converges faster as TxP decreases, whereas the variation of FAR is not significant.

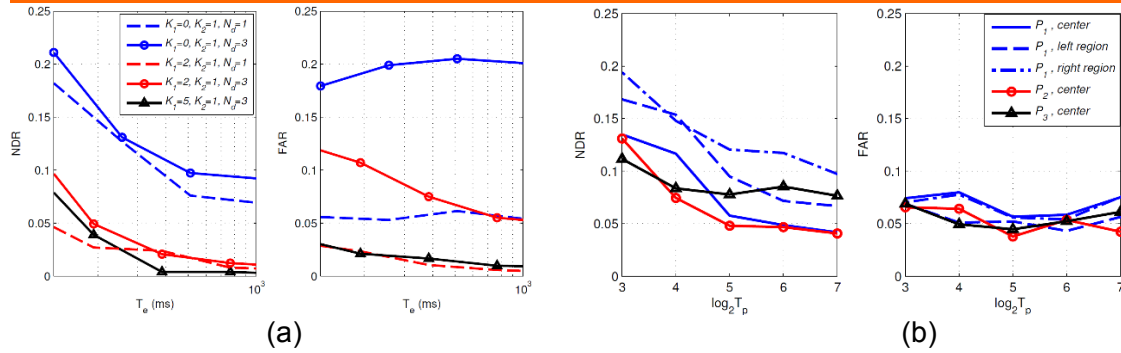


Figure 4-34 NDR and FAR as functions of execution time for different DOD algorithms

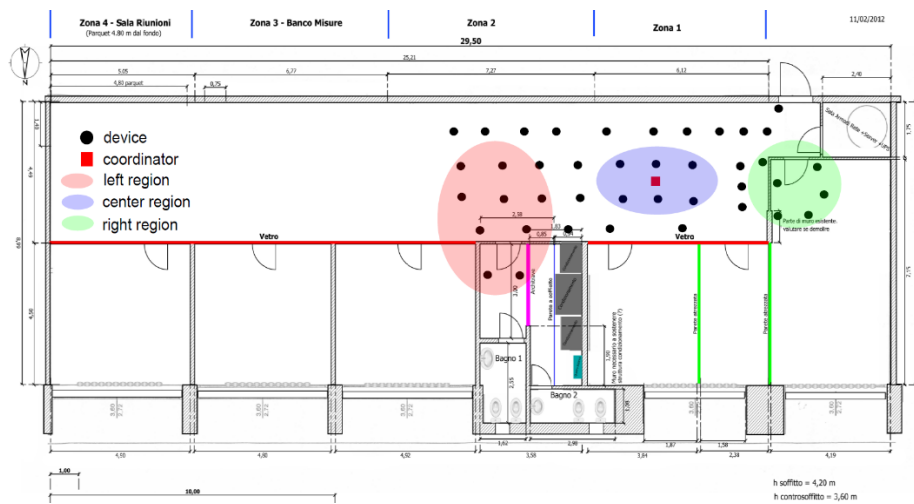


Figure 4-35 Node distribution in WiLab

References

- [1] W. Li, F. Bassi, D. Dardari, M. Kieffer, G. Pasolini, "Low-Complexity Distributed Fault Detection for Wireless Sensor Networks", IEEE ICC'15, London, UK, 2015.
- [2] W. Li, F. Bassi, D. Dardari, M. Kieffer, G. Pasolini, "Iterative Distributed Outlier Detection for Wireless Sensor Networks: Equilibrium and Convergence Analysis", Accepted by 54th IEEE Conference on Decision and Control, 2015.
- [3] W. Li, F. Bassi, D. Dardari, M. Kieffer, G. Pasolini, "Distributed outlier detection for Wireless Sensor Networks", Submitted to IEEE Trans. on Signal and Information Processing over Networks, 2015.

4.3 Achievements of JRA#5 “Socially-Aware Protocols for Wireless Mesh Networks”

4.3.1 Introduction

Opportunistic networks consist of nodes moving around and occasionally coming into each other proximity. During the limited proximity time nodes can exchange data. This results in a data dissemination process usually governed by a replication-based mechanism similar to the epidemic information spreading. Epidemic models have been proposed in the literature to predict performance in opportunistic scenarios. However these models usually rely on the use of Ordinary Differential Equations (ODEs) obtained as limits of the Markov models to illustrate nodes' interactions and inter-contacts. In order to be treatable, inter-contact time distributions among nodes' are usually assumed to be exponential and modeled by using Markov chains. However, it has been shown in the literature that nodes' inter-contacts are power-law distributed with exponential tails. Accordingly, in this work we propose a theoretical framework to model epidemic information dissemination while coping with realistic inter-contact time distributions. Numerical results are obtained by considering realistic inter-contact traces collected at the last EUCNC 2014 event and integrating them in the analytical framework. Comparison between realistic traces used for identifying the inter-contact rate among nodes and theoretical models assess the validity of the framework.

4.3.2 Inter-Contact Time Distribution and Markov Model

It has been deeply discussed in the literature that inter-contact time distributions among nodes exhibit a dichotomy and are power-law distributed with an exponential decay. Accordingly in this paper an equivalent Markov chain is introduced to model the inter-contact time distribution between pairs of users when taking into account real traces. More specifically we consider N different exponential distributions which fit the power law inter-contact time distribution for different time scales. The value of the inter-contact rate λ_i is quantized into finite discrete levels. Transitions between levels are assumed to occur with exponential transition rates which depend on the current state. Accordingly the inter-contact rate is approximated by a continuous time Markov process. The state space consists of the set of quantized λ_i levels up to the maximum of N . The number of states and the transition rates are tuned to fit the real measured data. Based on the real measured data, there are infinite possible choices of the Markov model which can fit the model. The choice of the specific model has been done based on the will to preserve both simplicity in the model as well as generality. Accordingly, we have considered a complete Markov model, as the one shown in Figure 4-36 where transitions are possible between any pair of states i and j , provided that the transition rate l_{ij} from state i to j is such that $l_{ij} = l_i$, $\forall j \neq i$. By solving the standard system used to model continuous time Markov chains

$$\begin{cases} \pi Q = 0 \\ \sum_{i=1}^N \pi_i = 1 \end{cases}$$

where Q is the matrix of the transition rates and π is the array of the stationary state probabilities π_i , it is possible to completely characterize the Markov chain of the inter-contact rates.

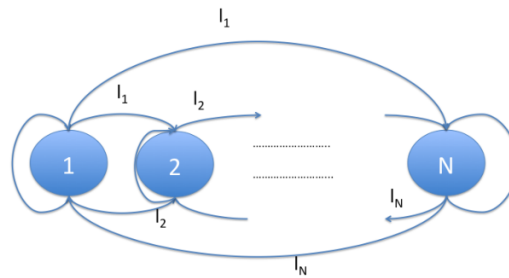


Figure 4-36: Markov model of the inter-contact rate process.

4.3.3 Epidemic Information Dissemination Model

To characterize data dissemination an opportunistic model is considered. In this case users move around and occasionally come into each other proximity. As nodes come into contact, they exchange data and, using this epidemic dissemination approach, the information is delivered at destinations. Without loss of generality, we assume that when two nodes meet, the transmission opportunity allows to transfer only one data packet per flow. In our model N network nodes and a source node are considered. We assume that a multicast dissemination is ongoing where D destination nodes have to receive the data packet. In order to avoid network overloading, a recovery is performed where a node, once delivered the packet to the destination, can delete the copy from its buffer to save storage space and prevent further infection. At the same time, the node saves information on the packet just delivered and consequently does not relay again the same packet in case it receives it again.

4.3.3.1 Notation

Let us denote as $I(t)$ the number of nodes which possess a data packet at time t ; moreover, let us indicate as $S(t)$ the number of susceptible nodes at time t , i.e. those nodes that are able to accept a packet since they did not yet received it. Moreover, $R(t)$ represents the number of nodes that have recovered at time t . A Markov chain model of an infectious process with susceptible, infected, and recovered states can be provided as shown in Figure 4-37.

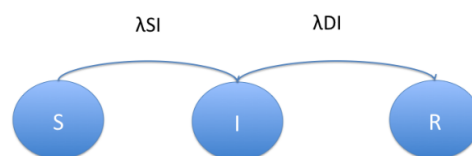


Figure 4-37: Markov model of the infection process.

The model is embedded with the underlying Markov chain of the inter-contact rate process discussed above. Accordingly, the Markov model of the infection process reduces to the one shown in Figure 4-38.

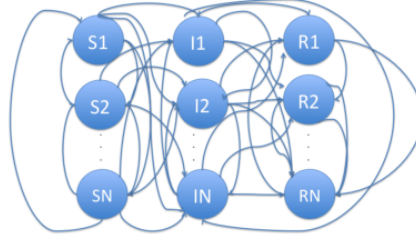


Figure 4-38: Modified Markov model of the infection process.

By considering the transitions from state $S_i(t)$ $i \in \{1, 2, \dots, N\}$ to state $I_j(t)$ $j \in \{1, 2, \dots, N\}$ and $R_k(t)$ $k \in \{1, 2, \dots, N\}$ it is possible to derive a system of ODEs as a fluid limit of the above Markov model. Hence it can be written:

$$\begin{cases} \frac{dS_i}{dt} = -l_{ii}S_i(t)I_i(t) - \sum_{j \neq i} S_i(t)I_j(t)l_{ij} + \sum_{j \neq i} S_j(t)l_{ji} - \sum_{j \neq i} S_i(t)l_{ij} \\ \frac{dI_i}{dt} = -l_{ii}S_i(t)I_i(t) - l_{ii}I_i(t)D + \sum_{j \neq i} S_j(t)I_i(t)l_{ji} - \sum_{j \neq i} I_j(t)l_{ji} - \sum_{j \neq i} I_i(t)l_{ij} \\ \frac{dR_i}{dt} = l_{ii}I_i(t)D + \sum_{i \neq j} D I_j(t)l_{ji} \end{cases}$$

where l_{ij} are the elements of the matrix \mathbf{Q} for the inter-contact rate process and $I_i(t)$, $R_i(t)$ and $S_i(t)$ are the number of infected nodes, recovered nodes and susceptible nodes in state i , respectively. In the following we denote as $I(t)$ the overall number of infected nodes, i.e. $I(t) = \sum_i I_i(t)$ and as $R(t)$ the overall number of recovered nodes, i.e. $R(t) = \sum_i R_i(t)$. In the above system of ODEs, the variation in the number of infected nodes is positively impacted by the rate at which susceptible nodes in the various states of the underlying Markov chain transit to the state $I_i(t)$, and negatively impacted by recovery of nodes as soon as they meet the destinations D or from transitions out of the state $I_i(t)$. Similarly, for the number of recovered nodes, the variation is positively impacted by nodes in states $I_h(t)$ with $h \in \{1, 2, \dots, N\}$ which transit to state $R_i(t)$ and negatively impacted by nodes which transit from state $R_i(t)$ to the other recovered states. Concerning the number of susceptible nodes in state i , $S_i(t)$, this value increases when transitions are executed from other susceptible states to i and decreases when transitions are executed to state $I_j(t)$ with $j \in \{1, 2, \dots, N\}$. By solving this ODEs system it is possible to study the variation in the number of recovered and infected nodes in the network.

4.3.4 Numerical Evaluation

In this section we will investigate how the information dissemination procedure works when considering the infection process enhanced with the underlying Markov chain of the inter contact rate process obtained by real traces. We will also compare the results obtained by using the theoretical framework upon assuming that inter- contact rate among nodes is exponentially distributed. To this purpose this section includes details for the characterization of the inter-contact time in realistic scenarios and the results of the numerical evaluation.

4.3.4.1 Realistic Inter-Contact Time Characterization

In order to realistically characterize the nodes inter- contact rate process we carried out an experiment. The aim of the experiment was to characterize the behavior of the attendees to a conference. The experiment was carried out during the last EuCNC 2014 conference held in Bologna. To collect the data, DataSens was exploited. This is one of the facilities offered by EuWIn; more specifically it is a platform consisting of 100 IEEE 802.15.4 compliant devices. The devices are TI CC2530 with a receiver sensitivity of -102 dBm. During the conference, a number of nodes between 35 and 45 were given to attendees, who carried them in their pocket/bag from 9 a.m. until 2 p.m. The experiment was repeated for three consecutive days. All devices transmitted a beacon every minute, with a transmit power set to 0 dBm. Each device, upon receiving a beacon from another node, records the following data:

- Identifier (ID) of the transmitting node.
- Timestamp, that is the instant when the beacon I received; the resolution of the timestamp was one minute and the time is calculated from the time instant when the device is switched on.
- Received Signal Strength Indication (RSSI), that is the power with which the beacon is received.

In order to elaborate the data and obtain the model of the inter-contact rate, a post processing phase was needed. The aim of the post processing operations is twofold: i) to find the distribution of the Inter-Contact Time (ICT) and ii) to find an approximation of this distribution as a weighted sum, with weights π_i , of N (negative) exponential distributions, with parameter λ_i , (WSE):

$$WSE_N(x) = \sum_{i=1}^n \pi_i \lambda_i e^{-\lambda_i x}$$

Subject to the condition

$$\sum_{i=1}^n \pi_i = 1$$

The first step of the post processing phase is to impose a threshold on the RSSI to avoid to consider encounters between people far from each other. To this aim we set the RSSI threshold for each node to the average RSSI evaluated from its log. Only encounters registered with an RSSI value higher than the RSSI threshold are kept. This per-node decision is motivated by the fact that every node works in different conditions (e.g., the node could be in the pocket or in the bag) and so it requires an ad- hoc setting decision rule on the RSSI threshold. In order to evaluate the inter-contact rate distribution we considered the three conference days and we observed that in all the cases the distribution function could be approximated by a Generalized Pareto Distribution (GPD), i.e.:

$$GPD(x|k, \sigma, \theta) = \left(\frac{1}{\sigma}\right) \left(1 + \frac{k(x-\theta)}{\sigma}\right)^{-1-\frac{1}{k}} \text{ for } k > 0, \theta < x$$

Accordingly we found an approximation of $GPD(x|k, \sigma, \theta)$, in the form reported in Eqs. (3) and (4) such that the Root Mean Squared Error (RMSE) is in the order of 10^{-2} . To this purpose we derived the parameters π_i and λ_i for a function of type WSE_3 since we experimentally observed that 3 exponential distributions are sufficient to model the ICT process. In Figure 4 we show the distribution function for the inter-contact time when considering experimental measurements and in Figure 5 we compare the fitting obtained and show the array of the values $L = [\lambda_1 \lambda_2 \lambda_3]$ and $\pi = [\pi_1 \pi_2 \pi_3]$.

4.3.4.2 Numerical Results

Based on the use of the above fitting of real traces, we were able to obtain the matrix \mathbf{Q} and the array $\mathbf{\Pi}$ and use them in the model described in eqs.(2). Accordingly in Figures 6 and 7 we show the evolution in the percentage of infected and the recovered nodes for different values of the number of destinations. Observe that upon increasing the number of destinations to be reached, this results as expected in a slight delay in the time needed to infect 100% of the nodes. However, the time delay is quite limited although increasing the number of destinations of almost 80% (from the case of 50 Destinations to 90 Destinations). Also we note that after 100% of nodes are infected, then a parallel increase in the number of recovered nodes is met till all nodes become recovered and the infection stops. It is obvious that a higher number of destinations implies a faster recovery process. In Figures 8 and 9 we report the curves obtained for the number of infected nodes and the recovered nodes in case an exponential distribution of inter-contact times is considered with an average rate $\lambda = 0.008$.

Observe that, the use of an exponential distribution implies a high degree of approximation in the performance of the dissemination process since less recovered nodes are obtained using the purely exponential modeling with a consequence that the dissemination process is in this case less aggressive compared to the realistic case. Indeed, in the realistic scenario, the dissemination procedure results very aggressive and almost 100% of nodes are recovered after less than 15 time units. This implies that the recovery is too prompt and nodes are recovered before they can spread the information. So the exponential modeling results too optimistic as compared to the realistic case. This was expected by considering indeed the specific features of the power law distribution.

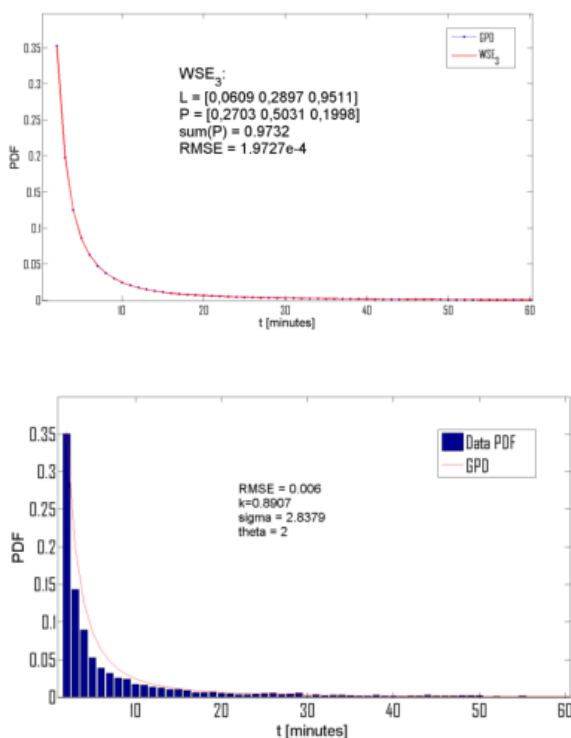


Figure 4-40: ICT distribution Function.

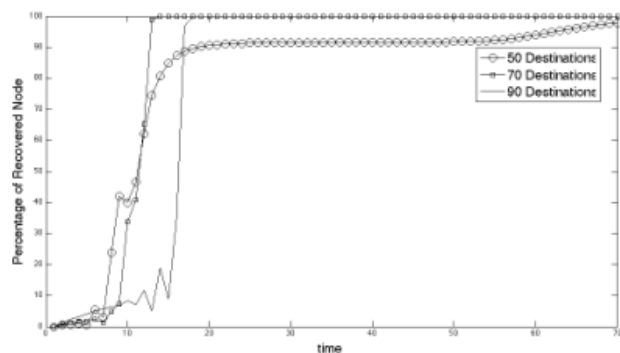


Figure 4-41: Percentage of recovered nodes as a function of time with $N_N = 100$ and D destinations.

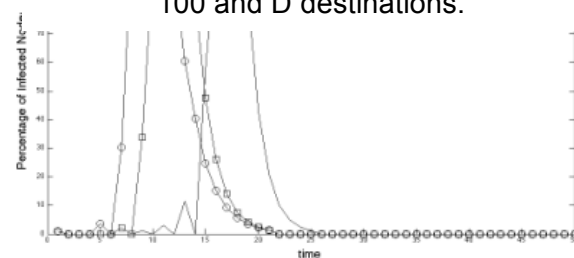


Figure 4-39: percentage of infected nodes as a function of time with $N_N = 100$ and D destinations.

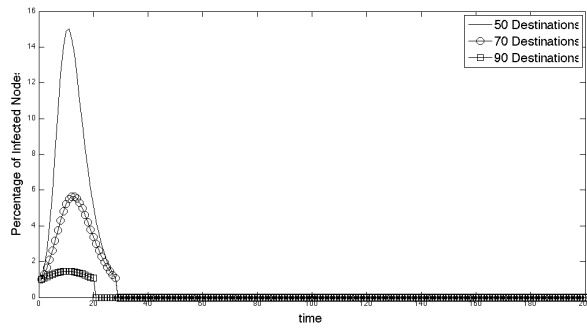


Figure 4-44: Number of infected nodes with the assumption of exponential ICT distribution with $N_N = 100$ and D destinations.

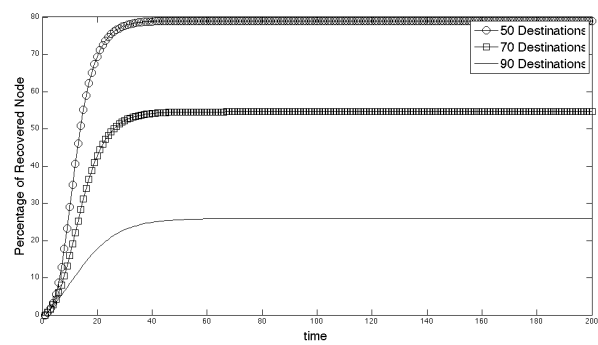


Figure 4-43: Number of recovered nodes with the assumption of exponential ICT distribution with $N_N = 100$ and D destinations.

4.3.5 Conclusions

In this paper we have provided an analytical model of epidemic information dissemination in opportunistic networks which consists of an underlying Markov chain obtained from realistic inter-contact time distributions. To this purpose we have considered a fluid Markov model which relies on an underlying Markov chain which models realistic inter-contact times among nodes by including the well known power-law with exponential tail behavior. Numerical results assess the effectiveness and realistic features caught by the model.

4.4 Achievements of JRA#6 "Testing IP-based Wireless Sensor Networks for the Internet of Things"

Several approaches have been considered by research community as possible enablers for the Internet of Things (IoT) implementation. This work presents the results obtained by testing and comparing the three different solutions reported in Section 2.5. Results show that SDWN is the best solution in static or quasi-static environments, while the performance degrades in highly dynamic conditions. However, ZigBee has a good re-activity to environmental changes.

4.4.1 Experimental Setup

We consider the following setup: a network consisting of 10 nodes (nodes 4, 6, 13, 17, 22, 25, 38, 43, 45, 51, see Figure 4-45). Node 53 at the end of the corridor, is used as the network coordinator.

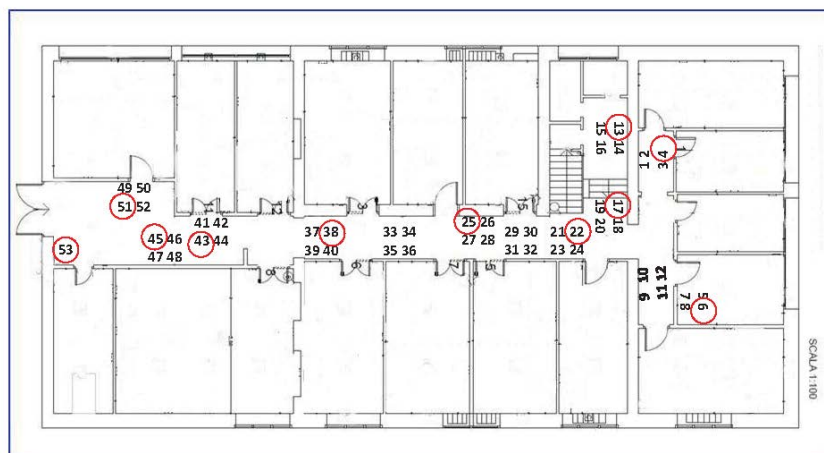


Figure 4-45: Flextop nodes map.

We consider a query-based application, where the coordinator periodically sends a query packet to one or several target nodes, and waits for the reply from it/them. Both queries and replies are data packets with a given payload that is the same in both cases, and we consider different payload sizes.

Two different communication configurations are evaluated: i) unicast, where the coordinator sends the query to one specific node that could be one, two or three hops far from the coordinator; and ii) multicast, where the coordinator queries contemporaneously a subset of nodes, and waits for replies from all of them.

As for the environmental conditions, all experiments were performed during the night, when no people were moving around, to avoid uncontrollable environmental changes and to ensure a fair comparison. However, in order to measure the level of reactivity of protocols to possible changes such as in real environments, we investigated results in *quasi-static* and *dynamic* conditions. In particular, experiments were still performed during the night, but we introduced the "disturbs" specified below. In the case of quasi-static environment, we emulated a day-like situation, where people move around, by letting two people walk along the corridor at a constant speed, following a pre-defined path. The comparison among protocols is still fair, since we reproduced exactly the same situation (same people, path and speed) during all experiments. This case is denoted as quasi-static, since only two people

were moving without creating huge obstacles and fast fading. In the case of dynamic environment, we emulated the movement of nodes leaving the network and possibly coming back, by switching off and on nodes at random instants. In particular, we implemented the following procedure: i) once a node switches on, it remains in this state for at least 5 seconds, after which it ii) generates a random and uniformly distributed delay between 0 and 10 seconds at the end of which iii) the node switches off for 1 second, and then it switches on again (back to step i)). The comparison among protocols is still fair, since the above described duty cycling is implemented in the tests identically. Moreover, the channel conditions could be considered as extremely dynamic, since nodes switches off frequently and at random time instants.

We consider the following performance metrics: i) packet loss rate (PLR); ii) round-trip-time (RTT); iii) overhead. In all experiments, the coordinator is sending one query every 300 ms toward the target node(s), and a total number of 5,000 queries are generated at the application layer. To compute the PLR, in each experiment we count the number of replies received at the coordinator, from each target node. The RTT is defined as the interval of time between the transmission of the query at the application layer of the coordinator, and the instant in which the reply is received at the application layer of the coordinator as well. Two definitions are used for the overhead: i) the ratio between the total number of packets transmitted in the network (being data packets transmitted for the first time or retransmitted, acknowledgement, or control packets), and the number of queries generated at the application layer of the coordinator; ii) the ratio between the total number of bytes transmitted in the network, and the number of bytes of information included in the generated replies.

4.4.2 Numerical Results

We firstly compare results among all considered protocols, for the case of static and quasi-static environments. In Figure 4-46, we show the RTT as a function of the number of hops for the case of 20 bytes of payload, unicast transmission and static environment. As expected, the RTT increases with the number of hops, since the packet has to pass through more routers. SDWN achieves better performance than other solutions, resulting in the lowest RTT in all cases. This is due to the fact that in SDWN, once the path between source and destination is established, forwarding at intermediate routers is very quick, since intermediate nodes just have to check the action corresponding to the received packet. In ZigBee and 6LoWPAN, instead, routing must be performed at each intermediate node, resulting in increased delay.

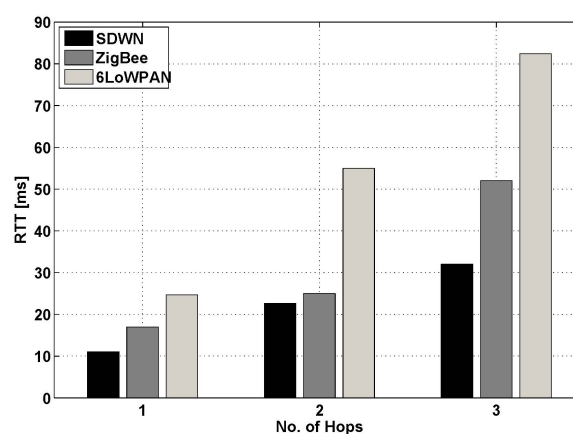


Figure 4-46: Unicast traffic: RTT as a function of the number of hops when transmitting 20 bytes of payload in static conditions.

In Table 4-1: Overhead: comparison among protocols. Table 4-1, we compare the overhead generated by the different protocols by considering a payload of 20 bytes, static environment, unicast traffic and different number of hops. As expected, the overhead is almost doubled by passing from 1 to 2 hops. Moreover, it is increasing by passing from SDWN to ZigBee and to 6LoWPAN solution. This is due to the fact that, in static conditions, SDWN keeps under control the number of packets transmitted during the path formation phase, while optimising paths reduces the number of data retransmissions.

Protocol	Packets:1 hop	Packets:2 hops	Bytes:1 hop	Bytes:2 hop
SDWN	2.6	5.6	2.5	5.6
Zigbee	4.7	8.7	6.5	11.4
6LoWPAN	6.2	9.5	10.9	16.8

Table 4-1: Overhead: comparison among protocols.

In Figure 4-47, we compare the RTT achieved in case of static and quasi-static environments, in particular considering the case of unicast traffic, 20 bytes of payload and 2 hops. As can be seen, in all cases, the RTT increases when passing from static to quasi-static conditions, due to: i) the need for searching for new paths when links become unreliable and/or ii) links being unreliable inducing more retransmissions, thus increasing the latency. However, in the considered environment, SDWN still remains the best solution, since the channel fading is still quite low and changes in the environment are slow, such that SDWN could properly react and work. Finally, note that 6LoWPAN shows the lowest performance degradation when passing from static to quasi-static, since the implemented Trickle algorithm allows for better adaptation of routing to environmental changes. Moreover, in the case of quasi-static environment, the PLR remains below 0.5% for all the cases, demonstrating the good reactivity of protocols when the environment changes slowly.

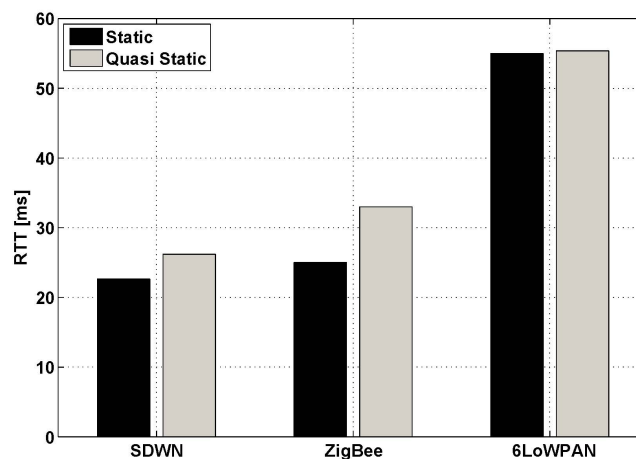


Figure 4-47: Unicast Traffic: RTT for the different protocols in the case of *static* and *quasi-static* conditions, setting 20 bytes of payload and 2 hops.

We also report results related to the multicast traffic, when triggering a multicast group that consists of nodes 4 and 6. Figure 4-48 shows the average RTT, averaged between the two triggered nodes, and the the average PLR. As can be seen, RTT is much higher than in the unicast case, especially for 6LoWPAN. The latter is due to an increase of the PLR that was below 0.5% in the case of unicast; losses due to collisions between data packets originating

from the nodes 4 and 6 that cause retransmissions, and consequently, the increase of delays. However, the multicast traffic increases the network throughput.

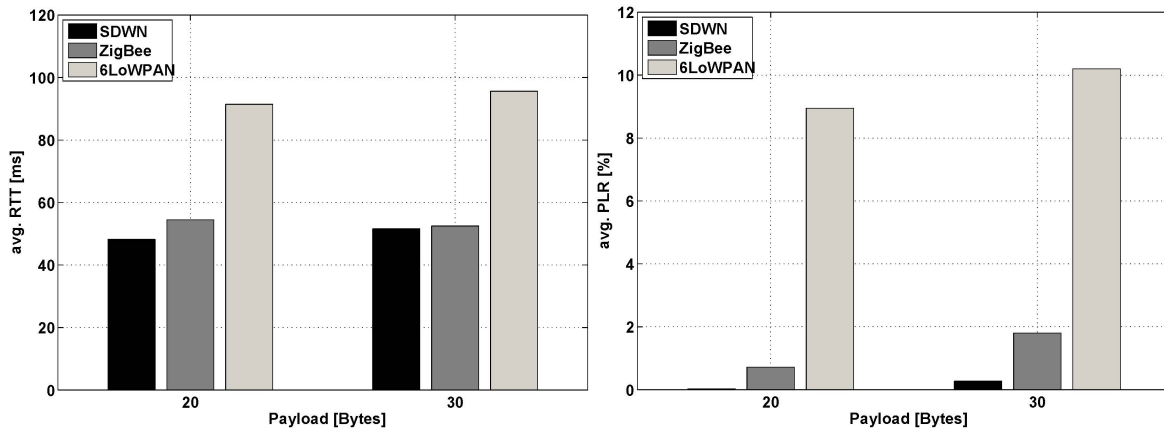


Figure 4-48: Multicast Traffic: Average RTT as a function of the payload size (on the left); Average PLR as a function of the payload size. (on the right).

We conclude by considering the case of dynamic environment, whose performance in terms of RTT and PLR are reported in Table 4-2. Results have been achieved by considering the unicast application, and 20 bytes of payload, where the coordinator queries node 4. In this case, a highly dynamic environment is emulated by making routers switched on and off at random instances of time. This requires nodes to refresh routes very quickly, because a router in a path already established could switch off and the source should search for a new relay for reaching the destination. All performance metrics have worsened both for ZigBee and SDWN. However, SDWN reaches a very large PLR, since most of the packets cannot find a proper route to reach the coordinator. The average RTT of SDWN still remains lower than in case of ZigBee, since when a packet manages to find a proper route with all routers switched on, forwarding is still very quick. This demonstrates that SDWN presents some issues in the case of highly dynamic environments, as expected.

Protocol	RTT [ms]	PLR [%]
SDWN	40	96
Zigbee	61	33

Table 4-2: Dynamic conditions: Comparing SDWN and ZigBee.

4.4.3 Conclusions

This work presents a comparison among different solutions for the IoT paradigm: ZigBee, 6LoWPAN and a software defined-based solution, SDWN, implementing a centralised routing. Results of an extensive measurements campaign performed over the EuWin laboratory are reported. Results show that in static and quasi-static conditions SDWN outperforms the other solutions, independently on the network size, payload size, traffic generated, and performance metric considered. However, when the situation is dynamic and there is a node mobility, a distributed solutions like ZigBee and 6LoWPAN could work better.

5. Annex II: Integration Document

5.1 Introduction

NEWCOM# is fostering through EuWIn the development of a new generation of researchers aiming at both fundamental and experimental research activities. The two mottos of EuWIn summarise the main scopes of EuWIn activities: “Fundamental Research Through Experimentation” and (more oriented to innovation and as such to the industry) “An Open Platform for Innovation”.

To achieve this general goal, a number of activities have been performed, which have involved all three components of EuWIn: the sites in Bologna, in Barcelona and at Sophia-Antipolis. Since these activities have been conducted jointly, they are reported through this Annex that is to be considered common to the three Deliverables D21.4, D22.4 and D23.4.

Though the NoE has come to an end, and as such its workplan is complete, EuWIn intends to foster its activities, philosophy and brand besides the temporal end of NEWCOM#.

This document describes the activities performed by EuWIn during the third year of the project, dedicated to the integration among the sites and the establishment of deeper and deeper levels of cooperation; moreover, it discusses the plans for the future.

The “*EuWIn Success Stories*” out of the activities performed during the three years of Newcom# will be highlighted.

5.2 Integration among the sites

The three sites perform activities that are, on purpose, related to separate fields of wireless communications. Nevertheless, some point of contacts have been sought, and some activities have been performed jointly, in order to achieve a higher degree of integration.

It is worth noting that there is no reason to seek for a “physical” integration among the three sites, besides the implementation of joint experimental works. In fact, the exchange of data among the sites does not require the use of specific high-capacity networking tools (like e.g. GEANT) or other infrastructural means to integrate the separate laboratories.

The rest of this subsection summarises the activities that were performed under this integrated approach among the three sites in the last year of the project.

- 1) Both EuWIn@UniBo and EuWIn@CTTC provide experimental platforms for indoor localisation. For this reason, JRA#1 has been maintained during year three, to consolidate the integration of software tools, and the achievement of a common open source platform for indoor localisation. Details are given in the body of D22.4.
- 2) In September 2015 the second EuWIn training school was organised at Sophia-Antipolis, with contributions from EuWIn@Eurecom and EuWIn@UniBo specifically dedicated to the interplay between experimentation and fundamental research.
- 3) The three sites of EuWIn have been presented jointly by the EuWIn Director in a number of meetings organised by EC during 2015 (in the context of the Expert Group of the Networld2020 platform and at concertation events).
- 4) All dissemination events during the three years of Newcom# have been participated by several EuWIn researchers, in all cases through a presentation given by the EuWIn Director (or a delegate) followed by three presentations, one per site.

- 5) EuWIn participated to EuCNC 2015 through a number of actions that were all organised jointly by the three sites: a demo stand, an experiment that involved about 40 attendees and a special session.
- 6) The plans for the future have been jointly devised by the three sites.

EuWIn Success Story 1: when Newcom# started, the three labs were performing research activities separately; after the three years of the project, the three labs have achieved durable integration, and agreed on the opportunity to pursue further dissemination of EuWIn philosophy through a plan that includes the definition of a common legal entity representing EuWIn future activities: EURACON, the European Association of Communications and Networking.

5.3 Dissemination

NEWCOM# Researchers during the third year of the project participated to the following three Dissemination events in order to disseminate EuWIn results and aims.

1) Dissemination event at Telecom Italia, Turin, Italy, February 26, 2015.

The following presentations related to Track 2 have been given:

The European Laboratory of Wireless Communications for the Future Internet

Roberto Verdone, CNIT/University of Bologna, Italy

OpenAirInterface Software Alliance and Cloud RAN

Raymond Knopp, CNRS/EURECOM

SDWN Approaches for the Internet of Things

Giacomo Morabito, CNIT/Univ. of Catania, and Chiara Buratti, CNIT/Univ. of Bologna

Radio Interfaces for Energy Efficiency and Interference Management

Miquel Payaro, CTTC

2) Dissemination event at Telefonica, Madrid, Spain, June 16, 2015.

The following presentations related to Track 2 have been given:

The European Laboratory of Wireless Communications

Roberto Verdone, CNIT/University of Bologna, Italy

Testbed for Experimentation on Positioning Systems

Miquel Payaro, CTTC, Spain

Testing IP-Based Wireless Sensor Networks for the Internet of Things

Melchiorre Danilo Abrignani, CNIT/University of Bologna, Italy

Network Architectures for the IoT

Roberto Verdone, CNIT/University of Bologna, Italy

3) Dissemination event at Ericsson, Stockholm, Sweden, May 4, 2015.

The following presentations related to Track 2 have been given:

The European Laboratory of Wireless Communications

Chiara Buratti (on behalf of Roberto Verdone), CNIT/University of Bologna, Italy

FBC-Related Experimental Activities at EuWIn@CTTC

Miquel Payaro, CTTC, Spain

Testbed for Experimentation on Positioning Systems

Miquel Payaro, CTTC, Spain

Testing IP-Based Wireless Sensor Networks for the Internet of Things

Chiara Buratti, CNIT/University of Bologna, Italy

Testing the Impact of WiFi Interference on Zigbee Networks

Chiara Buratti, CNIT/University of Bologna, Italy

Using OpenAirInterface on Generic Computing Equipment for Cloud RAN

Raymond Knopp, Florian Kaltenberger, EURECOM, France

Overall, the participation of the EuWIn researchers to these events was quite useful in order to set up collaborations with industries, receive information on research trends and disseminate the EuWIn brand. In particular, one of the three events (at Telecom Italia) produced further developments, as summarised in the following paragraph.

EuWIn Success Story 2: After the Newcom# dissemination event at Telecom Italia premises in 2015, based on the contacts established hereafter, EuWIn@UniBO organised a full day meeting in Bologna with the head of the Telecom Italia Future Center, Dr. Gian Paolo Balboni; Dr Balboni and three researchers from Telecom Italia, attended the meeting from Telecom Italia side. During the meeting all activities of EuWIn@UniBo were reviewed. After the meeting, two actions were taken:

- establishment of a collaboration finalised to open a PhD position at UniBO fully funded for three years by Telecom Italia, for research to be performed in the context of IoT at EuWIn@UniBO; this activity has been successfully closed and a PhD student has been selected, who will start on Nov. 1st 2015; he will pursue theoretical and experimental studies on emerging technologies for low power wide area networking for IoT applications;
- start of a discussion finalised to the possible duplication of the EuWIn FLEXTOP testbed at the premises of Telecom Italia Future Centre in Venice; this action is still ongoing.

5.4 Training

In September 2015 the third EuWIn School was organised. It was titled « Waveforms and Network Architectures for IoT in 5G » and it was held in Sophia-Antipolis on September 14-16. The focus of the school was on the aspects related to the impact of future IoT applications on 5G networks. In particular, the school dealt both from the theoretical and experimental viewpoint with 5G waveform design and network architectures. Two laboratory sessions were offered by EuWIn@Eurecom and EuWIn@UniBO. Lectures were given by researchers of EuWIn and invited speakers from TUD, Intel, CISCO and Alcatel-Lucent.

The school was attended by seventeen attendees. The list of names, with their affiliations, is reported below. As it is evident, though the number of attendees from the Newcom# community was very small, the school was very successful in attracting participants from industry, testifying the relevance of the topic addressed. The event itself, allowed to strengthen collaboration between EuWIn and the companies represented by the speakers and the attendees.

From the administrative viewpoint, the school was managed by EURACON. All information is available on the EURACON webpage <http://www.euracon.org/index.php/2013-02-12-09-41-49/wavenat5>.

EuWIn Success Story 3: EuWIn during the three years of Newcom# has become a reference entity able to coordinate the organisation of international schools including experimental sessions and attracting the interests of researchers from major industries.

First name	Last name	AFFILIATION
Kun	Chen Hu	Universidad Carlos III de Madrid
James	Birchall	University of Bristol
alireza	shams shafigh	CWC-university of oulu
Mohamed	Kamoun	Huawei
Loïg	Godard	Huawei
Raquel	Guerreiro Machado	Huawei
Eric	Simon	University of Lille1
Hamidreza	Khaleghi	b<>com
Jianqiang	Yang	Huawei Technologies France
Yoann	Roth	CEA
Iker	Sobron	University of the Basque Country (UPV/EHU)
Maria	Christopoulou	IASA-Wireless Systems Group
Francois	Taburet	Alcatel Lucent BellLabs France
Bruno	Mongazon	Alcatel-Lucent Bell Labs
Xiwen	Yiang	Eurecom
Kalyana	Gopala	Eurecom
Elena	Lukashova	Eurecom

5.5 Participation to EuCNC 2015

EuWIn participated very actively at EuCNC, the European Conference of Networks and Communications, organized in Paris, France, in June/July 2015, and participated by more than 500 attendees. In particular, the three EuWIn sites jointly organized a special session and a demo stand. Moreover, EuWIn@UniBO managed an experimental session during the days of the conference, which got the involvement of about 40 attendees. The snapshots below are taken from the final programme of the conference.

- Special Session: “European Platforms and Facilities for Experimentation Toward 5G”. Attended by nearly 50 participants.
- EuWIn Demo Stand. Based on a questionnaire distributed among attendees at the conference, it was very well received, being one of the best 20% appreciated stands.

SPS02 | EUROPEAN PLATFORMS AND FACILITIES FOR EXPERIMENTATION TOWARDS 5G

ROOM BERLIOZ | 11.00 - 12.30

SESSION CHAIR: MIQUEL PAYARÓ (CTTC, SPAIN)

OpenAirInterface: Open-source software radio solutions for 5G

Florian Kallenberger (Eurecom, France); Raymond Knopp (Institut Eurecom, France); Navid Nikaein, Dominique Nussbaum and Lionel Gauthier (Eurecom, France); Christian Bonnet (Institut Eurecom, France)

End-to-end 5G services via an SDN/NFV-based multi-tenant network and cloud testbed

Raul Muñoz (CTTC, Spain); Josep Mangués-Bafalluy (Centre Tecnològic de Telecomunicacions de Catalunya (CTTC), Spain); Nikolaos Bartzoudis, Ricard Vilalta and Ricardo Martínez (CTTC, Spain); Ramon Casellas (Centre Tecnològic de Telecomunicacions de Catalunya (CTTC), Spain); Nicola Baldo (Centre Tecnològic de Telecomunicacions de Catalunya (CTTC), Spain); José Núñez-Martínez (Centre Tecnològic de Telecomunicacions de Catalunya, Spain); Manuel Requena-Esteso (Centre Tecnològic de Telecomunicacions de Catalunya (CTTC), Spain); Oriol Font-Bach (Centre Tecnològic de Telecomunicacions de Catalunya, Spain); Marco Miozzo (Centre Tecnològic de Telecomunicacions de Catalunya (CTTC), Spain); Pol Henarejos (Centre Tecnològic de Telecomunicacions de Catalunya (CTTC), Spain); Ana Pérez-Neira (Centre Tecnològic de Telecomunicacions de Catalunya Castelfidels, Spain); Miquel Payaró (CTTC, Spain)

Ericsson's 5G Vision

Hugo M Tullberg (Ericsson Research, Sweden)

A Broadcast-Based Routing Protocol for Linear Wireless Networks: Design and Testing on EuWin

Chiara Buratti (University of Bologna, Italy); Andrea Stajkic (DEI, University of Bologna, Italy); Roberto Verdone and Parisa Hemmati (University of Bologna, Italy)

Virtualizing the Network Edge with Microservers

Filipe Manco and Kenichi Yasukata (NEC Europe Ltd., Germany); Joao Martins (NEC Europe Ltd, Germany); Felipe Huici (NEC Europe Ltd., Germany)

CHNICAL SESSIONS, SPECIAL SESSIONS

Excerpt from EuCNC'15 final programme: EuWin Special Session



RAYMOND KNOPP,
EURECOM, FRANCE

The exhibition is organized and supported by the European Laboratory of Wireless Communications for the Future Internet (EuWin) funded by the EC through the Network of Excellence in wireless com-

munications Newcom#. The EuWin facilities are distributed over three sites: at CTTC in Barcelona (Spain), at the University of Bologna (Italy) and at the Eurecom institute in Sophia-Antipolis (France). They are open for access by any scientist worldwide. EuWin is an integrated laboratory able to address, under a common environment, the various topics of wireless communication technologies for the future Internet. The laboratory activities aim at creating a new generation of researchers in wireless communications believing in the motto «Fundamental Research Through Experimentation». EuWin addresses topics and techniques related to the systems and networks that will drive the evolution of wireless communications in the years to come: LTE/4G, the Internet of Things, GNSS. Digital signal processing, radio access and network protocol aspects, are studied through the available lab facilities.

Demo: The Bologna IoT demo will access a site in Bologna remotely and demonstrate how sensor network experiments can be controlled from a remote location. EURECOM demo is centered around recent advances in the OpenAirInterface.org (OAI) platform. We will show an example of the use of OpenAir4G as a fully compliant 4G basestation using commercial terminals. We will also demonstrate how the OAI platform can be used to create so-called Cloud-RAN centralized processing for virtualizing basestations in a server platform.

EXHIBITIONS AND DEMOS

Excerpt from EuCNC'15 final programme: EuWin Exhibition Stand

5.6 Plans after Year 3

At the end of Year 2, as reported in the integration document annexed to D22.2, the plans for Year 3 of EuWIn were defined. In this section the common activities planned are recalled (in italic, with smaller character) one by one, and actual achievements are discussed.

- 1) *The three sites of EuWIn will be presented jointly by the EuWIn Director in **meetings organised by EC** (in the context of the Expert Group of the Network2020 platform and at concertation or similar events). It is expected that at least three presentations will be made during the third year of the project. The scope is to further increase visibility of EuWIn within the EC.* - This has happened in May 2015 at IEEE BlackSeaCom Conference, in June 2015 at IEEE ICC, in June 2015 at EuCNC, and through the active participation to the Expert Group of Network2020.
- 2) *All **dissemination events** during the third year of Newcom# will be participated by researchers presenting the three sites of EuWIn. The scope is to create additional follow-ups with large industries (contracts or collaborations with industry, joint participation in project proposals, etc).* - Done (see above)
- 3) *Contacts will be pursued during the third year of Newcom# with **SMEs** and associations of SMEs; in particular, CATAPULT, a British association involving a large number of SMEs in the field of ICT and IoT, has been recently contacted. There is the intention to meet in person in Bologna with the founder of the association. The scope is to better pursue the goal of supporting SMEs in innovation.* - There was no followup on the intention to meet the CATAPULT representative. On the other hand, EuWIn@UniBO was successful in contacting one (Italian) SME who took advantage of the FLEXTOP facility (see body of this Deliverable).

EuWIn Success Story 4: *EuWIn had already proved during the previous years to be able to attract interest of major companies towards the experimental facilities of the three sites. This was confirmed during the third year. However, during the third year it was also proved that EuWIn labs are effective in offering services to SMEs.*

- 4) *In February/March/April 2015 a **training school** will be organised in Sophia-Antipolis, specifically dedicated to the interplay between experimentation and fundamental research. The scope is to repeat the success of the school organised in 2013.* - The school was organised, in September 2015 (see above).
- 5) *EuWIn will participate to **EuCNC 2015** through a number of actions that will all be organised jointly by the three sites: a workshop, a demo stand and a special session will be proposed.* - Done (except for the workshop).
- 6) *EuWIn will act as one of the main drivers for the **survival of Newcom# community** after the end of the project; EuWIn will deliver specific plans for survivability after October 2015, during the dedicated internal workshop planned in Athens, on January 22, 2015. The scope is to let EuWIn act as a tool for keeping the Newcom# community spirit after the end of the NoE.* - This is discussed in the next section.

5.7 Plans for the Future

EuWIn intends to go beyond the temporal borders of Newcom#. This requires i) financial resources, and ii) a networking tool.

Financial resources to let the EuWIn lab continue their activities can be obtained mainly through two channels:

- 1) Industry contracts; owing to the nature of EuWIn, each site covers separate technological fields and therefore they pursue different industry contracts bringing to separate financial funding opportunities;

- 2) Projects financed by public bodies; EuWIn submitted during the third year of Newcom# a project proposal where the three legal entities were all present, proposing an integrated programme of activities. This proposal was not funded, but will be pursued again for the Call 2 of the H2020 Challenge on 5G. Other project submissions will be considered during 2016.

Besides the funds, it is clear to EuWIn researchers that a networking tool is needed, that is a framework incentivating and facilitating the organisation of regular meetings, training schools, student exchanges and the possibility to meet industry representatives. For this purpose a COST Action proposal was submitted during 2016, whose evaluation is still under process at time of writing this document. The Action proposed has an experimental track composed of three working groups that are based on EuWIn set of activities and experimental facilities. The Action would be an essential instrument for the survivability of EuWIn philosophy.

Assuming that the financial resources and networking framework will be both achieved, EuWIn will further its activities through a number of actions:

- Regular technical meetings (one or three per year depending on when the COST Action will be funded);
- Inclusion of new lab sites to extend the range of experimental facilities and fields of application;
- Organisation of one training school with experimental sessions every year;
- Exchange of students and researchers for short or long terms;
- Submission of project proposals for funding;
- Organisation of dissemination events at the premises of large industries;
- Possible other actions.

All these actions require a legal entity that manages the related financial resources, organises the events, meetings, etc. It is agreed that EURACON will act as the operational arm of EuWIn. Indeed, EURACON will be available for acting as Grant Holder responsible for the COST Action submitted, if accepted. This will facilitate the handling of all the actions mentioned above.

5.8 Conclusions

EuWIn has shown an ability to attract researchers and to succeed when presenting the three sites jointly, as they cover different aspects of wireless communications and are highly complementary. Large and small enterprises have shown to be interested in using EuWIn facilities.

A number of success stories can be mentioned for EuWIn. Three years ago, EuWIn was just a concept. At the end of Newcom# it is a reality. EuWIn intends to grow further after the end of Newcom#.

The website www.euwin.org will be the repository of all initiatives, after the end of Newcom#.

Comments and suggestions for the improvement of this document are most welcome and should be sent to:

project_office@newcom-project.eu



<http://www.newcom-project.eu>